Dynamics of flat membranes and flickering in red blood cells

Erwin Frey, David L. Nelson

Classification
Physics Abstracts
64.60Ht — 68.35Ja — 87.10+e

Dynamics of flat membranes and flickering in red blood cells

Erwin Frey and David R. Nelson

Lyman Laboratory of Physics, Harvard University, Cambridge, Massachusetts 02138, U.S.A.

(Received 3 June 1991, accepted in final form 20 August 1991)

Abstract. — A theory of the dynamics of polymerized membranes in the flat phase is presented. The dynamics of dilute membrane solutions is strongly influenced by long-ranged hydrodynamic interactions among the monomers, mediated by the intervening solvent. We discuss the renormalization of the kinetic coefficients for the undulation and phonon modes due to hydrodynamic "backflow" (Zimm behavior). The dynamics is also studied for free draining membranes (Rouse dynamics) corresponding to the Brownian dynamics method used in Monte Carlo simulations. The long time behavior of the dynamic structure factor is given by stretched exponentials with stretching exponents determined by the exponents of the elastic coefficients and the wave vector dependence of the Oseen tensor. We also study the dynamics of the thickness fluctuations in red blood cells (flicker phenomenon) taking into account the underlying polymerized spectrin skeleton. Qualitatively different dynamical behavior is predicted for spectrin skeletons isolated from their natural lipid environment.

1. Introduction.

There is now considerable theoretical and experimental interest in the statistical mechanics of membranes [1]. In contrast to linear polymers, surfaces fall into several universality classes [2], depending on rigidity, surface tension, and various microscopic constraints. One class of membranes that is being studied thoroughly is that of polymerized (or tethered) membranes [3]. These are two-dimensional analogs of linear polymer chains, and their study is a natural extension of polymer science. But, unlike polymers, which are always coiled up in three dimensions, tethered membranes are expected to exhibit a flat phase with long range order in the surface normals at low temperatures or high rigidity [4,5].

This flat phase has several unusual properties. First, the very existence of a flat $D = 2$ dimensional phase is surprising, since the theorem of Hohenberg and of Mermin and Wagner [6] forbids spontaneous symmetry breaking for two dimensional systems with a continuous symmetry. However, the coupling between the in-plane elastic degrees of freedom and the out-of-plane undulations introduces an effective long-ranged phonon-mediated interaction among the undulations [4]. The system therefore does not fall in the regime of validity of the Hohenberg-Mermin-Wagner theorem. Actually, the lower critical dimension found to leading order in a $1/d$-expansion is $D_{lc} = 2 - 2/d < 2$ [7,8], where d is the embedding dimension. Second, the classical theory of

elasticity is believed to break down due to the thermal out-of-plane fluctuations. The critical exponents, describing the nonclassical behavior of two-point correlation functions in the flat phase can be evaluated in approximation schemes such as the ϵ- or $1/d$-expansion [7-10]. The elastic constants are singular at long wave lengths, implying for example that the classical Hooke law is invalid in the flat phase.

The fluctuations in polymerized membranes were also studied numerically by Monte Carlo simulations [11-13] and molecular dynamics methods [14,15]. The results of these simulations suggest that simple triangulated tethered membranes with self-avoidance are always flat, due to the large entropically-induced bending rigidity. A high temperature crumpled phase has so far been observed only in the case of non self-avoiding "phantom" membranes [11].

From the experimental side there are several approaches to obtain tethered membranes. Polymerized networks appear naturally in a biological context [16,17]. An example of a biological tethered surface is the spectrin protein skeleton of erythrocytes, separated from its natural environment [18]. Polymerization of Langmuir films [19] and lipid bilayers [20] is another possibility, provided that the films can be made sufficiently flexible and placed in an appropriate solvent. A partial polymerization of phospholipid vesicles has been reported recently [21]. Recently thin membranes of graphite oxide have been synthesized by exfoiliating graphite [22]. Probing the conformation of these membranes using quasi-static light scattering shows that these graphitic membranes are folded into fractal objects with a fractal dimension $d_f \approx 2.5$ indicating that they may be in the crumpled phase.

Whereas the statics of polymerized membranes has been studied quite extensively, the dynamics of polymerized membranes have been studied only in the crumpled phase [3,23]. These investigations follow closely the concepts known from polymer dynamics [24]. The dynamics of linear polymers in a good solvent are fairly well understood. The simplest approach to polymer dynamics is to neglect the hydrodynamic interaction between different segments, which is known as the Rouse model [25]. It is known, however, that the long-ranged hydrodynamic interaction between different monomers, mediated by the intervening solvent, strongly influences the dynamics (Zimm dynamics) [26,27]. The dynamics of thickness fluctuations of red blood cells has been studied by Brochard and Lennon [28] using concepts known from the dynamics of surface waves [29].

In this paper we extend the equilibrium statistical mechanics of polymerized membranes in the flat phase to time-dependent quantities and study the dynamics of membranes in a solvent. Our purpose is to calculate transport coefficients like the diffusion constant of the center of mass motion (molecular weight dependence), correlation functions of the in-plane and out-of-plane modes and the dynamic scattering factor. The results are parametrized by the amplitudes and exponents of the (singular) equilibrium elastic constants and by transport coefficients.

We consider polymerized flat membranes, i.e., a system of atoms or monomers that are connected to form a regular two-dimensional array embedded in d-dimensional space (see Fig.1). What distinguishes the static universality class of tethered membranes from liquid membranes is their fixed connectivity. The statics of the flat phase of polymerized membranes is characterized by a non local wave vector dependent bending rigidity, and in-plane elastic constants [1,4,7,9]

$$\kappa(k) \sim k^{D-4+2\zeta}, \tag{1.1}$$

$$\lambda(k) \sim \mu(k) \sim k^{\omega} \tag{1.2}$$

In dynamics, additionally, the permeability of the membrane to solvent molecules plays a crucial role. Consider a simple model of beads of radius a connected by permeable tethers as shown in figure 1. We neglect for now internal elastic forces within the membranes. For very large mesh size the velocity of a particle is determined only by the local hydrodynamic forces acting on it.

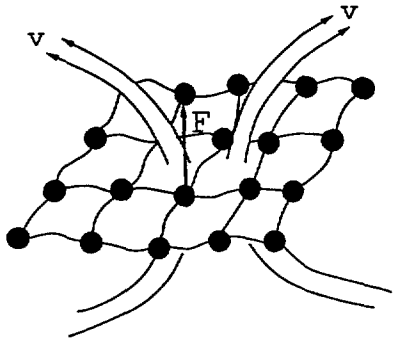

Fig. 1. — Simplified model of a polymerized membrane with beads connected by tethers. In fishnet-like polymers such as spectrin, these tethers are themselves linear polymer chains. A force F acting on a particle generates motion of the solvent indicated by the lines with arrows.

The bare viscous drag coefficients $\zeta_{u,h}$ relating the force on the particle to its in-plane (u) and out-of-plane (h) velocity is then simply $\zeta_{u,h} = 6\pi\eta a$, where η is the dynamic viscosity of the solvent. In general, however, the velocity of a particle depends in a complicated way on the forces acting on all other particles, because of the long range solvent velocity field generated by a localized force. The importance of this fluid backflow (hydrodynamic interaction) increases as the mesh size of the polymerized network decreases. If the membrane is completely impermeable to the fluid, the out-of-plane modes become slaved to the fluid motion perpendicular to the plane of the membrane. In this case the dynamics is very similar to that of surface waves [29]. The in-plane motion, however, should still show some slip relative to the liquid.

The above argument shows that the dynamics of polymerized networks are sensitive to the permeability of the membrane for solvent molecules. We can think of highly permeable and impermeable membranes as constituting two different dynamic universality classes of polymerized membranes. As an example of highly permeable polymerized membranes one may think of isolated spectrin networks, whereas red blood cells themselves (i.e., a lipid bilayer with a spectrin skeleton attached) represent impermeable membranes.

The bare friction of the membrane with the solvent is determined by the structure (permeability) of the membrane. We will show in section 2 that the hydrodynamic interaction between different monomers causes the renormalized mobility ($\mu \sim 1/\zeta$) to become inversely proportional to the wave vector k.

One explanation of this effect is that in the limit of long wavelength the motion of the membrane becomes slaved to the dynamics of the solvent. In this limit the dynamics becomes equivalent to a classical hydrodynamic problem with the boundary condition that the viscous stress of the solvent equals the elastic forces of the membrane. Upon neglecting all nonlinear effects one has for example $2\eta\frac{\partial v_z}{\partial z} - p = \kappa\frac{\partial^4 h}{\partial x^4}$ and $\frac{\partial h}{\partial t} = v_z$ for the out-of-plane fluctuations h, where $\vec{v}$ is the velocity field of the solvent and p the hydrostatic pressure. The expression for the in-plane motion are similar. A simple scaling analysis of these equations gives $\frac{\partial h(k,t)}{\partial t} \sim \frac{1}{k}\kappa k^4 h(k,t)$, i.e., the kinetic coefficient is inversely proportional to the wave vector k. One has to note, however, that the above consideration is based on the assumption that one can neglect nonlinear effects. In order to study those one has to use more sophisticated methods adapted from dynamic renormalization theory, which will be the subject of section 3.

The crossover from a wave vector independent friction ζ (Rouse dynamics, highly permeable membranes) to $\zeta \sim k$ (Zimm dynamics, impermeable membranes) is determined by the ratio of the (bare) friction coefficients ζ_u and ζ_h for the in-plane and out-of-plane motion and the dynamic viscosity η of the solvent. The crossover vector for the out-of-plane undulation mode is found to be

$$k_h = \frac{\zeta_h}{4\eta}, \tag{1.3}$$

and for the transverse and longitudinal phonon modes one obtains

$$k_\perp = \frac{\zeta_u}{2\eta}, \quad \text{and} \quad k_\parallel = \frac{\zeta_u}{4\eta} \tag{1.4}$$

For large viscosity η and/or for low friction ζ (high permeability) the crossover wave vectors become very small or even less than the smallest accessible wave vector $k_{min} = \pi/L$. In this case the dynamics is Rouse-like in the entire wave vector regime. In the opposite regime of very small viscosity and/or small permeability the crossover to Zimm dynamics sets in already for very large wave vectors. The location of the crossover point can thus be tuned by the viscosity of the solvent and/or the permeability of the membrane.

In section 3 we study the Rouse and Zimm dynamics by dynamic renormalization theory and find that the critical dynamic exponents characterizing the wave vector dependences of the characteristic frequencies $\Gamma_{u,h}$ for the (overdamped) undulation and the phonon modes are

$$\Gamma_h \sim k^{z_h}, \tag{1.5}$$

$$\Gamma_u \sim k^{z_u}, \tag{1.6}$$

where the dynamic critical exponents are determined by the wave vector dependences of the mobilities and the static exponents ζ and ω,

$$z_h = \begin{cases} 2 + 2\zeta & \text{for Rouse dynamics}, \\ 1 + 2\zeta & \text{for Zimm dynamics}, \end{cases} \tag{1.7}$$

and

$$z_u = \begin{cases} 2 + \omega & \text{for Rouse dynamics}, \\ 1 + \omega & \text{for Zimm dynamics}. \end{cases} \tag{1.8}$$

Here and in the remainder of the Introduction we specialize to a $D = 2$ dimensional membrane embedded in $d = 3$ dimensions. The corresponding expressions for general d and D can be found in the main text. Estimates of ζ from simulations are in the range $\zeta = 0.5 - 0.67$ [11,12,15], while ω is now believed to be rather small [30].

A quantity which can be directly measured in experiments is the dynamic structure factor. In the regime where the wave length is much larger than the linear dimension L of the membrane only the overall translational motion of the membrane can be seen. Then the dynamic structure factor shows an exponential decay

$$S(k,t) \sim \exp\left[-\mathcal{D}k^2 t\right], \tag{1.9}$$

where the diffusion constant is

$$\mathcal{D} \sim \begin{cases} 1/L^2 & \text{for Rouse dynamics,} \\ 1/L & \text{for Zimm dynamics.} \end{cases} \tag{1.10}$$

This result should be compared with $\mathcal{D} \sim L^{-4/5}$, obtained for Zimm dynamics in the crumpled phase [23].

In the opposite regime, where the wave length is much smaller than the linear dimension of the membrane, one is probing the internal motion of the membrane. The long time behavior of the dynamic structure factor is given by *stretched exponentials*

$$S(k,t) \sim \exp[-Ck^2t^{\alpha}], \tag{1.11}$$

if the scattering vector lies in or orthogonal to the membrane plane. For out-of-plane scattering vector the stretching exponent is given by $\alpha_{\text{Rouse}} = 2\zeta/(2+2\zeta)$ in the regime of Rouse dynamics and $\alpha_{\text{Zimm}} = 2\zeta/(1+2\zeta)$ in the Zimm regime, where ζ is the roughness exponent. For in-plane scattering vector we let $\alpha \to \beta$, where $\beta_{\text{Rouse}} = \omega/(2+\omega)$ and $\beta_{\text{Zimm}} = \omega/(1+\omega)$. Since the exponent ω, describing the renormalization of the phonon modes, is supposed to be a small number, the latter decay represents an enormous stretching which approximates an algebraic decay. For the special case $\omega = 0$ the static structure factor has power law singularities with a temperature dependent exponent analogous to the behavior of two dimensional solids. The time dependence is characterized by an algebraic decay, which is half as fast as the spatial decay for Rouse dynamics and equally fast for Zimm dynamics.

An important application of the dynamics of flat membranes are the thermal thickness fluctuations of red blood cells. The membrane of an erythrocyte essentially consists of a lipid bilayer (believed to be in a liquid phase) with a spectrin polymer network attached to the inner layer through proteins. The presence of the spectrin implies that unlike the phospholipid component of a biological membrane, the composite red blood cell membrane exhibits a shear modulus.

Under normal physiological conditions the red blood cells show a remarkable flicker phenomenon, which can be seen by phase contrast microscopy [28]. This flicker due to thermal fluctuations of the cell thickness.

Recently the spectrin skeleton of erythrocytes has been separated from their natural environment [18]. These isolated spectrin networks differ from the composite red blood cell not only in the magnitude of their elastic constants but also -and more importantly- in their permeability for solvent molecules. Whereas the permeability of the red blood cell is mainly determined by the flow through small protein channels, the isolated spectrin network is highly permeable for solvent molecules. As argued above the permeability of the membrane determines the location of the crossover from Rouse to Zimm dynamics. Hence we expect qualitatively different behavior for isolated spektrin networks as opposed to red blood cells as a consequence of their different permeability and elastic properties.

In section 5 we consider a simplified model of two membranes, separated by an average distance d and neglecting edge effects. We find the following crossover scenario for the thermal *thickness fluctuations*: For *highly permeable membranes*, like the isolated spectrin network there is a crossover from Rouse to Zimm behavior at a wave vector $k_{\text{h}} = \zeta_{\text{h}}/4\eta$. As a consequence of hydrodynamic screening effects this is followed by a reentrant crossover to Rouse dynamics when $kd \leq 1$. The Zimm behavior isrestricted to a wave vector regime $\zeta_{\text{h}}/4\eta > k > 1/d$. For highly permeable membranes this becomes a very narrow regime or even vanishes if $k_{\text{h}} < 1/d$.

A completely different crossover scenario is obtained for *impermeable* membranes, like the composite red blood cell. There one has to distinguish between large and small ratio of stretching to bending energy y. For $y >> 1$, which is the case for red blood cells, one obtains a crossover from Zimm dynamics with a kinetic coefficient proportional to $1/k$ to a kinetic coefficient proportional

to k^2 when $kd \leq 1$. In the regime $y << 1$ the linewidth shows a crossover from Zimm dynamics to a kinetic coefficient proportional to k. The results for the case of a very large ratio y of stretching to bending energy reduce to the results of Brochard and Lennon [28] for fluid like membranes provided we assume a liquid-like roughness exponent $\zeta = 1$. But, in addition to the lipid bilayer there is also a spectrin network attached to the bilayer leading to a solid-like structure of the composite object. This implies that there is a crossover from fluid- to solid-like behavior which has observable static [30] as well as dynamical consequencies.

The crossover scenario of the fluctuations of the difference of the *in-plane* modes is similar to that of the thickness fluctuations in the case of highly permeable membranes, whereas for impermeable membranes the crossover is from Zimm to Rouse dynamics. The in-plane modes have up to now not been studied experimentally. It would be interesting to design experiments which measure the in-plane dynamics of membranes.

Whereas the crossover of the relative modes is characterized by a change in the wave vector dependence, the center of mass modes for phonons and undulations show an enhancement of the amplitude by a factor of two in passing from $kd >> 1$ to $kd << 1$.

We thus conclude that the crossover scenario, upon passing from $kd << 1$ to $kd >> 1$, depends sensitively on two factors, the permeability of the membrane and the ratio of stretching to bending energy. This becomes evident if one considers the two extreme cases (i) an impermeable fluid ($\zeta = 1$) lipid bilayer (with $y >> 1$) [28] and (ii) polymerized ($\zeta \approx 0.5$) isolated spectrin networks with high permeability. The line width for the flicker modes are $\Gamma_h^{(i)} \sim k^6$ and $\Gamma_h^{(ii)} \sim k^3$, respectively, i.e., they differ by three powers in the wave vector!

The remainder of the paper is organized as follows: In section 2 we introduce the Langevin equations of motion describing the coupled dynamics of the membrane-solvent system. Using the functional integral formulation of Janssen [31] and de Dominicis [32] we define a generating functional for the dynamic correlation and response functions. By integrating out the solvent velocity fields we find an effective fluid-mediated long ranged hydrodynamic interaction between different segments of the surface. In a preaveraging approximation (similar to that used for linear polymer chains), the hydrodynamic interaction leads to a renormalization of the kinetic coefficients. The renormalization of the resulting effective model is studied in section 3. It is found that the dynamic exponents can be expressed entirely in terms of the static exponents and the exponent of the kinetic coefficients. The scaling properties and the wave vector and time dependence of the dynamic structure factor is discussed in section 4. In section 5 we discuss the hydrodynamic modes of two flat membranes. This can be considered as a model system for red blood cells. In the Appendix we show how to obtain the scaling functions from a self consistent dynamical theory which is similar to mode coupling theory.

2. Model.

In this section we introduce equations of motion for the dynamics of a membrane in its flat phase suspended in a fluid solvent. We shall describe the dynamics of a membrane-solvent system by a set of coupled Langevin equations.

Apart from the nonlinear coupling between the bending and stretching modes, which determine the static properties of flat membranes, the dynamics of dilute membrane solutions are strongly influenced by long-ranged hydrodynamic interactions, mediated by the intervening solvent. We assume that the dynamics is purely dissipative since the contributions of the inertial terms for membranes in a solvent can be neglected for sufficiently large times. The Langevin dynamics

for the membrane conformation $\vec{R}(\mathbf{s},t)$ ($\mathbf{s}$ is an internal coordinate parametrizing monomer positions) states that the friction force $\zeta^0_{ij}\left[\partial_t R_j(\mathbf{s},t) - g_0 v_j[\vec{R}(\mathbf{s},t),t]\right]$ is balanced by the internal elastic forces of the membrane and the random forces proportional to $\Theta_i(\mathbf{s},t)$

$$\frac{\partial R_i(\mathbf{s},t)}{\partial t} = -L^0_{ij}\frac{\delta\mathcal{H}(\{\vec{R}\})}{\delta R_j(\mathbf{s},t)} + g_0 v_i[\vec{R}(\mathbf{s},t),t] + \Theta_i(\mathbf{s},t)\,, \tag{2.1}$$

where the matrix of the bare friction coefficients ζ^0_{ij} per unit area is the inverse matrix of the bare Onsager kinetic coefficients L^0_{ij}. The values of these friction coefficients depend on the permeability of the membrane to solvent molecules. As discussed in the Introduction, the permeability should depend on the mesh size. If the membrane is completely impermeable to the fluid the Onsager coefficients for the out-of-plane motion are zero and these modes become slaved to the fluid motion perpendicular to the reference plane of the membrane. The in-plane motion, however, should still show some slip relative to the liquid.

$\mathcal{H}(\{\vec{R}\})$ is the free energy functional (made dimensionless by dividing by k_BT) for the membrane conformation field $\vec{R}(s,t)$. In the flat phase the excitations can be decomposed into transverse undulations, h, and internal phonon modes, $\mathbf{u}$

$$\vec{R}(\mathbf{s},t) = m\,[\mathbf{s} + (\mathbf{u}(\mathbf{s},t), h(\mathbf{s},t))]\,. \tag{2.2}$$

The quantity m is the order parameter and characterizes the extension factor, i.e., the ratio between the actual linear size of the fluctuating membrane and its size at $T = 0$. The internal space of the membrane is characterized by a D-dimensional vector $\mathbf{s}$. Note that vectors $\mathbf{s}$ in the internal space are written in boldface, while vectors $\vec{R}$ in the d-dimensional external space are denoted with an arrow.

The free energy functional is given by [4,5]

$$\mathcal{H} = \int \mathrm{d}^D s\left[\frac{1}{2}\lambda_0 u^2_{ii} + \mu_0 u^2_{ij} + \frac{\kappa_0}{2}(\vec{\nabla}^2 h_\alpha)^2\right] \tag{2.3}$$

with the strain tensor

$$u_{ij} = \frac{1}{2}\left[\partial_i u_j + \partial_j u_i + \partial_i h_\alpha \partial_j h_\alpha\right]\,. \tag{2.4}$$

The coefficient κ_0 is the bare bending rigidity, and λ_0 and μ_0 are the bare Lamé coefficients. The parameter g_0 is the bare strength of the hydrodynamic interaction, i.e., the coupling to the solvent velocity field $v_i[\vec{x},t]$. This coefficient is arbitrary, and may be taken to be unity as is required for a Galilean invariant model. One should also note that mode-coupling coefficients of the streaming type (here g_0) are not renormalized in general [33,34]. If one sets g_0 equal to zero, equation (2.1) describes the free draining (Rouse) model for the membrane dynamics.

The dynamics of the solvent velocity field is described by fluctuating hydrodynamics. The relevant hydrodynamic equations of motion for the fluid velocity are those of low Reynolds number hydrodynamics. The solvent dynamics is thus described by linearized Navier-Stokes equations, which incorporate friction forces due to the membrane and the random thermal velocity fluctuations in the fluid

$$\frac{\partial v_i(\vec{x},t)}{\partial t} = \nu_0\vec{\nabla}^2 v_i(\vec{x},t) - \frac{g_0}{\rho_0}\int \mathrm{d}^D s\frac{\delta\mathcal{H}(\{\vec{R}\})}{\delta R_i(\mathbf{s},t)}\delta(\vec{x} - \vec{R}(\mathbf{s},t)) - \frac{1}{\rho_0}\frac{\partial p}{\partial x_i} + \zeta_i(\vec{x},t)\,. \tag{2.5a}$$

Here ν_0 is the kinematic solvent viscosity, p is the hydrostatic pressure, ρ_0 is the fluid mass density and $\vec{\zeta}(\vec{x},t)$ are random thermal forces driving the system to equilibrium as $t \to \infty$. It is assumed that the fluid is incompressible, i.e.,

$$\vec{\nabla} \cdot \vec{v} = 0\,, \tag{2.5b}$$

which is an adequate assumption for describing low frequency dynamics of the membrane. Inertial terms are also unimportant at low frequencies. The random forces $\vec{\Theta}(\mathrm{s},t)$ and $\vec{\zeta}(\vec{x},t)$, necessary for producing the correct equilibrium distribution function for both the membrane and the solvent in the long time limit, are Gaussian white noise sources with zero means and variances

$$< \Theta_i(\mathrm{s},t)\Theta_j(\mathrm{s}',t') > = 2L^0_{ij}\delta(\mathrm{s}-\mathrm{s}')\delta(t-t')\,, \tag{2.6a}$$

$$< \zeta_i(\vec{x},t)\zeta_j(\vec{x}',t') > = -2\eta_0\vec{\nabla}^2\delta(\vec{x}-\vec{x}')\delta(t-t')\delta_{ij}\,, \tag{2.6b}$$

where $\eta_0 = \nu_0\rho_0$ is the dynamic viscosity and we have set $k_\mathrm{B}T = 1$. It can be shown that correlations calculated from the above Langevin equations satisfy the usual fluctuation-dissipation relations.

The equations of motion for the fluid (2.5) can be formally solved by first transforming into k-space

$$\frac{\partial v_i(\vec{k},t)}{\partial t} + \nu_0 k^2 v_i(\vec{k},t) = -\frac{g_0}{\rho_0}\int \mathrm{d}^D s \frac{\delta\mathcal{H}}{\delta R_i(\mathrm{s},t)} e^{-i\vec{k}\cdot\vec{R}(\mathrm{s},t)} + \frac{ik_i}{\rho_0} p(\vec{k},t) + \zeta_i(\vec{k},t)\,, \tag{2.7a}$$

$$i\vec{k}\cdot\vec{v}(\vec{k},t) = 0\,, \tag{2.7b}$$

and then eliminating the pressure in equation (2.7a) using the incompressibility condition (2.7b). One finds

$$\frac{\partial v_i(\vec{k},t)}{\partial t} + \nu_0 k^2 v_i(\vec{k},t) = P^{\mathrm{T}}_{ij}(\hat{k})\left[\zeta_j(\vec{k},t) - \frac{g_0}{\rho_0}\int \mathrm{d}^D s \frac{\delta\mathcal{H}}{\delta R_j(\mathrm{s},t)} \mathrm{e}^{-i\vec{k}\cdot\vec{R}(\mathrm{s},t)}\right]\,, \tag{2.8}$$

where

$$P^{\mathrm{T}}_{ij}(\hat{k}) = \delta_{ij} - \frac{k_i k_j}{k^2} \tag{2.9}$$

is the transverse projection operator. The formal solution of equation (2.8) is

$$v_i(\vec{k},t) = \int_{-\infty}^{t} \mathrm{d}t' \mathrm{e}^{-\nu_0 k^2(t-t')} P^{\mathrm{T}}_{ij}(\hat{k})\left[\zeta_j(\vec{k},t) - \frac{g_0}{\rho_0}\int \mathrm{d}^D s \frac{\delta\mathcal{H}}{\delta R_j(\mathrm{s},t')} \mathrm{e}^{-i\vec{k}\cdot\vec{R}(\mathrm{s},t')}\right]\,. \tag{2.10}$$

This shows that, whenever a force (2nd term in the square brackets on the right hand side of Eq. (2.10)) acts on a surface element of the membrane, the result is a distorted velocity field in the whole fluid. This "backflow" decreases only slowly (inversely proportional to the distance) and drives other elements of the membrane into motion. As we will see, this hydrodynamic interaction leads to a drastic renormalization of the kinetic coefficient. Note also that only the transverse noise $\zeta^{\perp}_i(\vec{k},t) = P^{\mathrm{T}}_{ij}\zeta_j(\vec{k},t)$ enters since the fluid is incompressible.

As in discussions of polymer chain dynamics [24], we assume that the typical solvent relaxation times are much shorter than those of the membrane conformation and make the replacement [35]

$$e^{-\nu_0 k^2(t-t')} \to \frac{2}{\nu_0 k^2}\delta(t-t'). \tag{2.11}$$

In this Markovian approximation the formal solution of the fluid equation simplifies to

$$v_i(\vec{k},t) = \frac{2}{\nu_0 k^2} P_{ij}^{T}(\hat{k})\left[\zeta_j(\vec{k},t) - \frac{g_0}{\rho_0}\int d^D s \frac{\delta\mathcal{H}}{\delta R_j(s,t)} \exp\left(-i\vec{k}\cdot\vec{R}(s,t)\right)\right]. \tag{2.12}$$

Therefore the hydrodynamic interaction term $g_0\vec{v}[\vec{R}(s,t),t]$ in the Langevin equation for the membrane becomes

$$\begin{aligned} g_0 v_i[\vec{R}(s,t),t] = g_0 \int \frac{d^d k}{(2\pi)^d}\frac{2}{\nu_0 k^2} P_{ij}^{T}(\hat{k})\Big[\zeta_j(\vec{k},t)\exp\left(-i\vec{k}\cdot\vec{R}(s,t)\right) \\ -\frac{g_0}{\rho_0}\int d^D s' \frac{\delta\mathcal{H}}{\delta R_j(s',t)}\exp\left(-i\vec{k}\cdot\left(\vec{R}(s,t)-\vec{R}(s',t)\right)\right)\Big]. \end{aligned} \tag{2.13}$$

One way to proceed would be to insert these expression into the Langevin equation for the membrane and study the dynamics directly in terms of the equations of motion as in the renormalization group approach to dynamic critical phenomena [36,37]. Here we formulate instead a path integral description for the membrane-solvent dynamics, a method which has also been successfully used to study critical dynamics.

Before analyzing the effects of the nonlinearity in the static Hamiltonian and the hydrodynamic interaction let us consider a simple case first. If the membrane is completely impermeable for the fluid and there is no slip for the in-plane motion of the membrane, the dynamics of the membrane becomes completely slaved to the dynamics of the solvent, i.e.

$$\frac{\partial h}{\partial t} = v_z(t), \quad \text{and} \quad \frac{\partial u_i}{\partial t} = v_i(t), \quad (i = x, y).$$

Neglecting effects from the roughness of the membrane surface and the nonlinearities in the static Hamiltonian (see Sect. 2.2) the dynamic problem is equivalent to a classical hydrodynamic problem with the boundary conditions that the viscous stress of the fluid equals the elastic forces of the membrane

$$2\eta\frac{\partial v_z}{\partial z} - p = \kappa_0\frac{\partial^4 h}{\partial x^4}, \qquad \eta\left(\frac{\partial v_x}{\partial z} + \frac{\partial v_z}{\partial x}\right) = -(\lambda_0 + 2\mu_0)\frac{\partial^2 u_x}{\partial x^2},$$

where for simplicity we are considering the case $v_y = 0$. These boundary conditions determine the coefficients A and B in the solution of the linear Navier-Stokes equation

$$v_x = \left(ikAe^{kz} - lCe^{lz}\right)e^{ikx-i\omega t}, \qquad v_z = \left(kAe^{kz} + ikCe^{lz}\right)e^{ikx-i\omega t},$$

$$p = -i\omega\rho A e^{kz} e^{ikx-i\omega t}$$

Without even solving these equations explicitely one can recognize from a pure scaling analysis that the equations of motion for the undulation and phonon modes are of the form

$$\frac{\partial h(k,t)}{\partial t} \sim \frac{1}{k}\kappa_0 k^4 h(k,t),$$

$$\frac{\partial u_x(k,t)}{\partial t} \sim \frac{1}{k}(\lambda_0 + 2\mu_0)k^2 h(k,t).$$

Compared to a Rouse model with wave vector independent kinetic coefficient the above analysis shows that in the regime where the membrane dynamics is slaved by the solvent motion the kinetic coeffients become inversely proportional to k. Here this is a consequence of the solution of a classical hydrodynamic problem with boundary conditions similar to the well known problem of capillary waves. The physical reason is the long ranged nature of the hydrodynamic backflow as explained above.

In the next section we formulate a path integral description of the dynamics, which allows us to study the effects of static and dynamic nonlinearities and to scrutinize the approximations made in the above hydrodynamic analysis. Furthermore, this formalism allows us to study the general case of a D-dimensional membrane embedded in d dimensions.

2.1 PATH INTEGRAL FORMULATION AND DYNAMIC FUNCTIONAL. — In order to implement dynamic renormalization theory in a way analogous to static critical phenomena we need a functional which generates the perturbation expansion for the frequency dependent correlation and response functions, which follows from the equations of motion. We shall use a functional integral formulation [31,32,38,39] which converts the Langevin equations into a dynamic functional with one additional field [39]. The idea is that instead of solving the Langevin equations (2.1) and (2.8) for the membrane field $\vec{R}(\mathrm{s},t)$ and solvent velocity field $\vec{v}(\vec{x},t)$ in terms of the random forces $\vec{\Theta}(\mathrm{s},t)$ and $\vec{\zeta}_\perp(\vec{x},t)$ and then averaging over the Gaussian weight

$$\begin{aligned} w(\{\Theta\},\{\zeta_\perp\}) \sim & \exp\left[-\frac{1}{4}\int \mathrm{d}t \int \mathrm{d}^D s \Theta_i(\mathrm{s},t)(L^{-1})_{ij}\Theta_j(\mathrm{s},t)\right] \\ & \times \exp\left[-\frac{1}{4}\int \mathrm{d}t \int \mathrm{d}^d x \vec{\zeta}_\perp(\vec{x},t)(\eta_0(i\vec{\nabla})^2)^{-1}\vec{\zeta}_\perp(\vec{x},t)\right], \end{aligned} \tag{2.14}$$

one can eliminate the random forces in favour of the conformation variables for the membrane and the velocity fields of the solvent by introducing a path probability density $W(\{R\},\{v\})$ via

$$W(\{R\},\{v\})\mathcal{D}[R]\mathcal{D}[v] = w(\{\Theta\},\{\zeta_\perp\})\mathcal{D}[\Theta]\mathcal{D}[\zeta_\perp]. \tag{2.15}$$

Furthermore, it is convenient to perform a Gaussian transformation in order to "linearize" the dynamic functional. This is accomplished by introducing response fields $\tilde{R}$ and $\tilde{v}$ [31,32,38,39]

$$W(\{R\},\{v\}) = \int \mathcal{D}[i\tilde{R}] \int \mathcal{D}[i\tilde{v}] \exp\left[J(\{R\},\{\tilde{R}\},\{v\},\{\tilde{v}\})\right]. \tag{2.16}$$

For more details on the general formalism we refer the reader to references [31,32,38,39]. The dynamical functional is given by

$$J(\{R\},\{\tilde{R}\},\{v\},\{\tilde{v}\}) = J_{\text{fluid}}(\{R\},\{\tilde{R}\},\{v\},\{\tilde{v}\}) + J_{\text{membrane}}(\{R\},\{\tilde{R}\},\{v\},\{\tilde{v}\}), \tag{2.17}$$

where

$$\begin{aligned} J_{\text{fluid}} = \int_k \int \mathrm{d}t \Big[& \tilde{v}_i(\vec{k},t)\eta_0 k^2 P^{\mathrm{T}}_{ij}(\hat{k})\tilde{v}_j(-\vec{k},t) - \tilde{v}_i(\vec{k},t)P^{\mathrm{T}}_{ij}(\hat{k})\left[\partial_t - \nu_0 k^2\right] v_j(-\vec{k},t) \\ & - \frac{g_0}{\rho_0}\tilde{v}_i(\vec{k},t)P^{\mathrm{T}}_{ij}(\hat{k}) \int \mathrm{d}^D s \frac{\delta \mathcal{H}}{\delta R_j(\mathrm{s},t)} \exp\left(i\vec{k}\cdot\vec{R}(\mathrm{s},t)\right)\Big], \end{aligned} \tag{2.18a}$$

and

$$J_{\text{membrane}} = \int \mathrm{d}^D s \int \mathrm{d}t \Big[\tilde{R}_i(\mathrm{s},t) L^0_{ij} \tilde{R}_j(\mathrm{s},t) - \tilde{R}_i(\mathrm{s},t) \Big[\partial_t R_i(\mathrm{s},t) + L^0_{ij} \frac{\delta \mathcal{H}}{\delta R_j(\mathrm{s},t)} \Big] , + g_0 \tilde{R}_i(\mathrm{s},t) P^T_{ij}(\hat{k}) v_j[\vec{R}(\mathrm{s},t),t] \Big] . \tag{2.18b}$$

We have used the notation $\int_k = \int \mathrm{d}^d k/(2\pi)^d$ and $\int_\omega = \int \mathrm{d}\omega/2\pi$. Since the dynamical functional is quadratic in the solvent velocity fields, they can be integrated out exactly. One finds

$$\exp\Big[J_{\text{eff}}(\{R\},\{\tilde{R}\})\Big] = \int \mathcal{D}[i\tilde{v}] \int \mathcal{D}[v] \exp\Big[J(\{R\},\{\tilde{R}\},\{v\},\{\tilde{v}\})\Big] = \text{const.} \times \exp\Big[J_{\text{Rouse}}(\{R\},\{\tilde{R}\}) + J_{\text{Hydro}}(\{R\},\{\tilde{R}\})\Big] . \tag{2.19}$$

The first term,

$$J_{\text{Rouse}}(\{R\},\{\tilde{R}\}) = \int \mathrm{d}^D s \int \mathrm{d}t \Big[\tilde{R}_i(\mathrm{s},t) L^0_{ij} \tilde{R}_j(\mathrm{s},t) - \tilde{R}_i(\mathrm{s},t) \Big(\partial_t R_j(\mathrm{s},t) + L^0_{ij} \frac{\delta \mathcal{H}}{\delta R_j(\mathrm{s},t)} \Big) \Big] , \tag{2.20a}$$

corresponds to the dynamics of a free draining membrane. In analogy to the polymer case we call it the Rouse part [25] of the dynamical functional. The second term is more conveniently written in Fourier space

$$J_{\text{Hydro}}(\{R\},\{\tilde{R}\}) = = \frac{g_0^2}{2\rho_0} \int_k \int_\omega (Q_i(\vec{k},\omega), -\tilde{Q}_i(\vec{k},\omega))(\mathbf{A}^{-1}(\vec{k},\omega))_{ij} (Q_j(-\vec{k},-\omega), -\tilde{Q}_j(-\vec{k},-\omega))^{\mathrm{T}} , \tag{2.20b}$$

and describes the hydrodynamic interaction between different parts of the membrane. Here

$$(\mathbf{A}^{-1}(\vec{k},\omega))_{ij} = \frac{1}{\omega^2 + (\nu_0 k^2)^2} \begin{pmatrix} 0 & i\omega + \nu_0 k^2 \\ -i\omega + \nu_0 k^2 & 2\eta_0 k^2 \end{pmatrix} P^{\mathrm{T}}_{ij}(\hat{k}) , \tag{2.21}$$

and we have defined the "generalized" Fourier transforms

$$Q_i(\vec{k},t) = \int \mathrm{d}^D s \frac{\delta \mathcal{H}}{\delta R_i(\mathrm{s},t)} \exp\Big[-i\vec{k}\cdot\vec{R}(\mathrm{s},t)\Big] , \tag{2.22a}$$

and

$$\tilde{Q}_i(\vec{k},t) = \int \mathrm{d}^D s \tilde{R}_i(\mathrm{s},t) \exp\Big[-i\vec{k}\cdot\vec{R}(\mathrm{s},t)\Big] . \tag{2.22b}$$

Explicitely one finds in the Markovian approximation (see Eq. (2.11))

$$J_{\text{Hydro}}(\{R\},\{\tilde{R}\}) = \int_k \frac{g_0^2}{\eta_0 k^2} \int \mathrm{d}^D s \int \mathrm{d}^D s' \int \mathrm{d}t \Big[\tilde{R}_i(\mathrm{s},t) P^{\mathrm{T}}_{ij}(\hat{k}) \tilde{R}_j(\mathrm{s}',t) - \tilde{R}_i(\mathrm{s},t) P^{\mathrm{T}}_{ij}(\hat{k}) \frac{\delta \mathcal{H}}{\delta R_j(\mathrm{s}',t)} \Big] \mathrm{e}^{-i\vec{k}\cdot(\vec{R}(\mathrm{s},t) - \vec{R}(\mathrm{s}',t))} \tag{2.23}$$

This can also be written as

$$J_{\text{Hydro}}(\{R\},\{\tilde{R}\}) = \int \mathrm{d}t \int_{\mathbf{q}} \tilde{R}_i(\mathbf{q},t) K_{ij}(-\mathbf{q}) \left[\tilde{R}_j(-\mathbf{q},t) - \frac{\delta \mathcal{H}}{\delta R_j(\mathbf{q},t)} \right] \tag{2.24}$$

where

$$K_{ij}(\mathbf{q}) = \int_k \int \mathrm{d}^D s \int \mathrm{d}^D s' P_{ij}^{\mathrm{T}}(\hat{k}) \frac{1}{\eta_0 k^2} \mathrm{e}^{-i\mathbf{q}\cdot(\mathbf{s}-\mathbf{s}')} \exp\left[-i\vec{k} \cdot (\vec{R}(\mathbf{s},t) - \vec{R}(\mathbf{s}',t)) \right] . \tag{2.25}$$

2.2 PREAVERAGING APPROXIMATION. — One way to analyze the hydrodynamic interaction is to replace the operator $K_{ij}(\mathbf{q})$ by its averaged value $< K_{ij}(\mathbf{q}) >$, the so called Oseen tensor. This preaveraging approximation is frequently used in polymer physics and is due to Kirkwood and Riseman [27] and Zimm [26]. As in reference [15], we assume that the static fluctuations discussed in reference [4,7,9] have been incorporated into renormalized, wave vector dependent elastic constants. Accordingly, we make the replacements $\kappa_0 \to \kappa_{\mathrm{R}}(q) \sim q^{D-4+2\zeta}$, $\mu_0 \to \mu_{\mathrm{R}}(q) \sim q^{\omega}$, and $\lambda_0 \to \lambda_{\mathrm{R}}(q) \sim q^{\omega}$ in equation (2.3). Upon averaging with respect to this fully renormalized static Hamiltonian one finds

$$\begin{aligned} < K_{ij}(\mathbf{q}) > = L^D \int_{\tilde{k}} \int \mathrm{d}^D(\mathbf{s}-\mathbf{s}') P_{ij}^{\mathrm{T}}(\hat{k}) \frac{1}{\nu_0 k^2} \mathrm{e}^{-i(\mathbf{q}+\mathbf{k}_\perp)\cdot(\mathbf{s}-\mathbf{s}')} \\ \times \exp\left[-2k_l k_m \int_{\mathbf{p}} \chi^{lm}(\mathbf{p}) \sin^2(\mathbf{p}\cdot(\mathbf{s}-\mathbf{s}')/2) \right] , \end{aligned} \tag{2.26}$$

where the static susceptibility matrix $\chi^{lm}(\mathbf{p})$ reads

$$\chi_{\mathrm{h}}(\mathbf{p}) = \chi^{zz}(\mathbf{p}) = < h(\mathbf{p}) h(-\mathbf{p}) > \approx \frac{1}{\kappa p^{D+2\zeta}} \tag{2.27a}$$

for the undulation modes with the roughness exponent ζ and

$$\chi_{\mathrm{u}}^{ij}(\mathbf{p}) \approx P_{ij}^{\mathrm{L}}(\mathbf{p}) \frac{1}{(\lambda+2\mu)p^{2+\omega}} + P_{ij}^{\mathrm{T}}(\mathbf{p}) \frac{1}{\mu p^{2+\omega}} \tag{2.27b}$$

for the phonon modes with the exponent ω. As shown by Aronovitz and Lubensky [9], the exponents ζ and ω are not independent, but obey instead the important scaling relation

$$\zeta = \frac{1}{4}(4 - D + \omega) . \tag{2.28}$$

The coefficients κ, λ and μ are wave vector independent renormalized amplitude factors. By a straightforward scaling analysis of equation (2.26) one finds

$$\begin{aligned} < K_{ij}(\mathbf{q}) > = q^{d_{\infty}-2} L^D \int_{\mathbf{z}_\perp} \int_{z_\parallel} \int \mathrm{d}^D x P_{ij}^{\mathrm{T}}(\hat{z}) \frac{1}{\eta_0 (z_\perp^2 + z_\parallel^2)} \mathrm{e}^{-i(\hat{e}_{\mathbf{q}}+\mathbf{z}_\perp)\cdot\mathbf{x}} \\ \times \exp\left[-\frac{1}{\kappa} A_h(\hat{e}_{\mathbf{s}}) |\mathbf{x}|^{2\zeta} z_\parallel^2 q^{2-2\zeta} \right] \\ \times \exp\left[-\left(\frac{1}{\lambda+2\mu} A_{\mathrm{L}}^{lm}(\hat{e}_{\mathbf{s}}) + \frac{1}{\mu} A_{\mathrm{T}}^{lm}(\hat{e}_{\mathbf{s}}) \right) |\mathbf{x}|^{\omega+(2-D)} z_\perp^l z_\perp^m q^{D-\omega} \right] , \end{aligned} \tag{2.29}$$

where $d_{co} = d - D$ is the co-dimension and the amplitude factors

$$A_h(\hat{e}_s) = \int d^D y\, y^{-D-2\zeta}(1 - \cos(\mathbf{y} \cdot \hat{e}_s)) \tag{2.30}$$

and

$$A^{ij}_{L,T}(\hat{e}_s) = \int d^D y\, y^{-2-\omega}(1 - \cos(\mathbf{y} \cdot \hat{e}_s)) P^{ij}_{L,T}(\mathbf{y}) \tag{2.31}$$

depend on $\hat{e}_s = (s - s')/|s - s'|$. $k_\perp$ and $k_{||}$ denote the in-plane and out-of-plane components of the wave vector $\vec{k}$ respectively. This scaling analysis is valid for $0 < \zeta < 1$ and $0 < \omega + 2 - D < 2$. Otherwise the p-integration in equation (2.26) depends explicitly on the lower or upper bounds of the integral. With these restrictions the leading wave vector dependence of the Oseen tensor in the flat phase is given by

$$< K_{flat}(q) > \sim q^{d_{co}-2} \tag{2.32}$$

Currently accepted values of ζ for $d = 3$, $D = 2$ are in the range $0.5 \leq \zeta \leq 0.67$ [4,15,30,40] while it is believed that $\omega > 0$ [9,15,40]. The long wave length behavior of the Oseen tensor is thus independent of the precise values of the static critical exponents ζ and ω. Furthermore, it does not depend on the internal and external dimension separately, but instead solely on the co-dimension. From this analysis the hydrodynamic interaction can be regarded as relevant for $d_{co} < 2$, marginal for $d_{co} = 2$ and irrelevant for $d_{co} > 2$. The marginal case corresponds to rod like polymers ($D = 1$) in $d = 3$ dimensions with bending rigidity.

The above result for the Oseen tensor is equivalent to replacing the term $\vec{R}(s,t) - \vec{R}(s',t)$ in the hydrodynamic interaction, equation (2.23), by its average value $s - s'$, which is non zero due to the fact that the membrane is flat on average. This approximation corresponds to neglecting some correlation effects in the hydrodynamic interaction. The $1/q$-behavior of the Oseen tensor reflects the broken symmetry of the flat phase. In the crumpled phase the average value of $\vec{R}(s,t) - \vec{R}(s',t)$ is zero, but there are non trivial renormalizations due to self-avoidance (see below).

The dynamic properties of a solution of self-avoiding crumpled membranes has recently been studied by Mutukumar [23] using a preaveraged Oseen tensor approach. He finds for the Oseen tensor

$$< K_{crumpled} > \sim q^{-D-\nu(2-d)}, \tag{2.33}$$

where

$$\nu = \frac{D+2}{d+2} \tag{2.34}$$

is the exponent of the mean square distance between two points of the manifold,

$$< [\vec{R}(0) - \vec{R}(L)]^2 > = |L|^{2\nu}, \tag{2.35}$$

found in a self consistent approach for the excluded volume effect. This result for the exponent ν agrees with a Flory type argument [3], and with the value found by numerical simulations [3], $\nu = 0.80 \pm 0.05$. A first order ϵ-expansion gives $\nu = 0.556$ [11,41]. If the Flory value for ν ($\nu = 4/5$, for $d = 3$, $D = 2$) is used the wave vector dependence of the Oseen tensor is given by $< K_{crumpled} > \sim q^{-6/5}$, which is close to what we found for the flat phase. But, the physical basis is completely different.

In the crumpled phase the wave vector dependence of the Oseen tensor depends crucially on the renormalization of the "elastic" coefficients due to self-avoidance or equivalently on the fractal dimension $d_f = 2/\nu \approx 2.5$ of the crumpled object. One should note that without self avoidance (i.e., for "phantom" membranes) the radius of gyration scales as $R_g \sim \sqrt{\ln L}$ implying that the Oseen tensor would scale as $< K_{\text{crumpled}} > \sim q^{-2}$, which is completely different from the above result with self-avoidance.

In the flat phase the wave vector dependence is dominated by the fact that the membrane is a flat object. Actually, summarizing both results, equations (2.32) and (2.33) the wave vector dependence can be written in terms of the fractal dimension as

$$< K_{\text{crumpled}} > \sim q^{-D+D(d-2)/d_f} \tag{2.36}$$

In the flat phase, the leading wave vector dependence of the Oseen tensor can be obtained by making the replacement

$$\exp\left[-i\vec{k}\cdot(\vec{R}(\mathbf{s},t)-\vec{R}(\mathbf{s}',t))\right] \to \exp\left[-i\vec{k}\cdot\langle\vec{R}(\mathbf{s},t)-\vec{R}(\mathbf{s}',t)\rangle\right] \tag{2.37}$$

in the hydrodynamic interaction, equation (2.24). With this approximation, the resulting dynamical functional corresponds to the following set of effective Langevin equations for the phonon modes

$$\frac{\partial u_i(\mathbf{k},t)}{\partial t} = -D_{ij}(\mathbf{k})\frac{\delta\mathcal{H}}{\delta u_j(-\mathbf{k},t)} + \tilde{\Theta}_i(\mathbf{k},t)\,, \tag{2.38a}$$

and the undulation modes

$$\frac{\partial h(\mathbf{k},t)}{\partial t} = -L(\mathbf{k})\frac{\delta\mathcal{H}}{\delta h(-\mathbf{k},t)} + \tilde{\Theta}_h(\mathbf{k},t)\,, \tag{2.38b}$$

where the hydrodynamically renormalized kinetic coefficients are given by

$$D_{ij}(\mathbf{k}) = D_0\delta^{ij} + \frac{g_0^2}{2\eta_0\, k}\left(\delta^{ij} - \frac{1}{2}\frac{k_i k_j}{k^2}\right)\,, \tag{2.39a}$$

$$L(\mathbf{k}) = L_0 + \frac{g_0^2}{4\eta_0\, k}\,. \tag{2.39b}$$

The covariance of the noise terms are

$$< \tilde{\Theta}_i(\mathbf{k},t)\tilde{\Theta}_j(\mathbf{k}',t') >= 2D_{ij}(k)\delta(\mathbf{k}+\mathbf{k}')\delta(t-t')\,, \tag{2.40a}$$

$$< \tilde{\Theta}_h(\mathbf{k},t)\tilde{\Theta}_h(\mathbf{k}',t') >= 2L(k)\delta(\mathbf{k}+\mathbf{k}')\delta(t-t')\,. \tag{2.40b}$$

The hydrodynamic interaction leads to kinetic coefficients proportional to $1/k$ in the long wave length limit, reflecting the long-ranged nature of the fluid-mediated interaction.

At the harmonic level one can already discuss the crossover from Rouse to Zimm behavior (for sufficiently permeable membranes), i.e., a crossover in the kinetic coefficients from a wave vector independent constant to the singular $1/k$-behavior. As can be inferred from equations (2.39), the crossover wave vector for the out-of-plane undulations is given by

$$k_h = \frac{g_0^2}{4\eta_0 L_0} \tag{2.41}$$

For the phonon modes we find

$$k_\perp = \frac{g_0^2}{2\eta_0 D_0}\,, \tag{2.42a}$$

and

$$k_\parallel = \frac{g_0^2}{4\eta_0 D_0} \tag{2.42b}$$

Note that the crossover from Rouse to Zimm behavior for the longitudinal phononsis shifted by a factor of 2 with respect to the crossover for the transverse phonons, i.e., $k_\perp/k_\parallel = 2$. The physical reason for this shift is that the fluid is incompressible. Therefore the coupling of the longitudinal membrane phonons to the fluid motion is weaker than for the transverse ones. The crossover from Rouse to Zimm dynamics is determined by the ratio of the friction coefficients of the membrane and the viscosity of the solvent. Hence for membranes with a high friction coefficient, or in other terms low permeability for solvent molecules, and/or a solvent with a small viscosity the crossover to Zimm dynamics already starts at large wave vectors. This implies that a membrane with a small permeability can be described by Zimm dynamics throughout the entire wave vector regime.

On the other hand, if the membrane is highly permeable for solvent molecules (small friction coefficient) and/or the solvent has a large viscosity the crossover from Rouse-like to Zimm-like dynamics is shifted to very small wave vectors. The crossover wave vector may even become less than the smallest accessible wave vector $k_{\min} = \pi/L$, where L is the linear dimension of the membrane. Then the dynamics is Rouse-like over the entire wave vector regime.

3. Renormalization of the effective model and self consistent theory.

In this section we study the renormalization of the effective model introduced in the preceding section. To cover both cases, Rouse and Zimm dynamics, we take the kinetic coefficients to be of the form

$$L_0(\mathbf{p}) = L_0 p^a\,, \tag{3.1a}$$

and

$$D^0_{ij}(\mathbf{p}) = (D^{\mathrm{L}}_0 P^{\mathrm{L}}_{ij}(\mathbf{p}) + D^{\mathrm{T}}_0 P^{\mathrm{T}}_{ij}(\mathbf{p}))p^a \tag{3.1b}$$

The exponent $a = 0$ corresponds to Rouse and $a = d_{\mathrm{co}} - 2$ ($a = -1$ for $D = 2$ and $d = 3$) to Zimm dynamics. While the Zimm dynamics is the realistic model for a single membranes with a small permeability for solvent molecules, the Rouse model is important for the following reasons. (i) As discussed in the preceding section there is a crossover from Rouse to Zimm behavior by passing from smaller to larger wave vectors. This crossover may even be absent for membranes with a large permeability and/or a solvent with a large viscosity. (ii) The Brownian dynamics method used in Monte Carlo simulations actually corresponds to Rouse dynamics. (iii) The hydrodynamic interaction is relevant only if the co-dimension $d_{\mathrm{co}} = d - D < 2$, it is marginal for $d_{\mathrm{co}} = 2$, and irrelevant for $d_{\mathrm{co}} > 2$ (see Sect. 2.2).

Now we study the consequences of the vertex structure and fluctuation-dissipation relations on the renormalization of the kinetic coefficients. The dynamic functional for the effective Langevin equations reads

$$J(\{R\},\{\tilde{R}\}) = J_0(\{R\},\{\tilde{R}\}) + J_{\mathrm{int}}(\{R\},\{\tilde{R}\})\,, \tag{3.2}$$

where the harmonic part of the dynamical functional is given by

$$J_0(\{R\},\{\tilde{R}\}) = \int_{\mathbf{p}}\int_{\omega}\left[j(\{h\},\{\tilde{h}\}) + j(\{u\},\{\tilde{u}\})\right], \tag{3.3}$$

with

$$j(\{h\},\{\tilde{h}\}) = -\frac{1}{2}(\tilde{h}^{\alpha}(\mathbf{p},\omega), h^{\alpha}(\mathbf{p},\omega))\mathbf{A}_{\mathrm{h}}^{\alpha\beta}(\mathbf{p},\omega)(\tilde{h}^{\beta}(-\mathbf{p},-\omega), h^{\beta}(-\mathbf{p},-\omega))^{\mathrm{T}} \tag{3.4}$$

for the bending modes and

$$j(\{u\},\{\tilde{u}\}) = -\frac{1}{2}(\tilde{u}^{i}(\mathbf{p},\omega), u^{i}(\mathbf{p},\omega))\mathbf{A}_{\mathrm{u}}^{ij}(\mathbf{p},\omega)(\tilde{u}^{j}(-\mathbf{p},-\omega), u^{j}(-\mathbf{p},-\omega))^{\mathrm{T}} \tag{3.5}$$

for the phonon modes. The tensors $\mathbf{A}_{\mathrm{h}}$ and $\mathbf{A}_{\mathrm{u}}$ are

$$\mathbf{A}_{\mathrm{h}}^{\alpha\beta}(\mathbf{p},\omega) = \delta^{\alpha\beta}\begin{pmatrix} -2L_0p^a & i\omega + L_0p^a(p^4+\tau_0p^2) \\ -i\omega + L_0p^a(p^4+\tau_0p^2) & 0 \end{pmatrix}, \tag{3.6}$$

and

$$\mathbf{A}_{\mathrm{u}}^{ij}(\mathbf{p},\omega) = \begin{pmatrix} -2A^{ij}(\mathbf{p}) & i\omega\delta^{ij} + B^{ij}(\mathbf{p}) \\ -i\omega\delta^{ij} + B^{ij}(\mathbf{p}) & 0 \end{pmatrix}, \tag{3.7}$$

with

$$A^{ij}(\mathbf{p}) = D_0^{\mathrm{L}}p^a P_{ij}^{\mathrm{L}}(\mathbf{p}) + D_0^{\mathrm{T}}p^a P_{ij}^{\mathrm{T}}(\mathbf{p}), \tag{3.8a}$$

and

$$B^{ij}(\mathbf{p}) = D_0^{\mathrm{L}}p^a(\lambda_0+2\mu_0)p^2P_{ij}^{L}(\mathbf{p}) + D_0^{\mathrm{T}}p^a\mu_0p^2P_{ij}^{\mathrm{T}}(\mathbf{p}). \tag{3.8b}$$

The transverse and longitudinal projection operators in the D-dimensional internal space are defined by

$$P_{ij}^{\mathrm{T}}(\mathbf{p}) = \delta^{ij} - \frac{p_ip_j}{p^2}, \tag{3.9a}$$

and

$$P_{ij}^{\mathrm{L}}(\mathbf{p}) = \frac{p_ip_j}{p^2} \tag{3.9b}$$

Note that the Onsager coefficients for the undulation modes L_0 and the phonon modes D_0 are in general different.

The interaction part of the dynamical functional consists of three parts, two 3-point vertices

$$\begin{aligned} J_{\mathrm{int}}^{3a} = i\delta^{\alpha\beta}\prod_{i=1}^{3}\int_{\mathbf{p}_i,\omega_i}\delta(\sum_{i=1}^{3}\mathbf{p}_i)\delta(\sum_{i=1}^{3}\omega_i)L_0p_1^a\Big(\mu_0\left[(\mathbf{p}_3\cdot\mathbf{p}_1)p_2^l + (\mathbf{p}_3\cdot\mathbf{p}_2)p_1^l\right] \\ +\lambda_0(\mathbf{p}_1\cdot\mathbf{p}_2)p_3^l\Big)\tilde{h}^{\alpha}(\mathbf{p}_1,\omega_1)h^{\beta}(\mathbf{p}_2,\omega_2)u^{l}(\mathbf{p}_3,\omega_3), \end{aligned} \tag{3.10}$$

$$J_{\rm int}^{3b} = \frac{i}{2}\delta^{\alpha\beta}\prod_{i=1}^{3}\int_{\mathbf{p}_i,\omega_i}\delta(\sum_{i=1}^{3}\mathbf{p}_i)\delta(\sum_{i=1}^{3}\omega_i)\left(\mu_0\left[(\mathbf{p}_3\cdot\mathbf{p}_1)p_2^l+(\mathbf{p}_3\cdot\mathbf{p}_2)p_1^l\right]+\lambda_0(\mathbf{p}_1\cdot\mathbf{p}_2)p_3^l\right)$$
$$\times[D_0^{\rm L}P_{lm}^{\rm L}(\mathbf{p}_3)+D_0^{\rm T}P_{lm}^{\rm T}(\mathbf{p}_3)]p_3^a h^\alpha(\mathbf{p}_1,\omega_1)h^\beta(\mathbf{p}_2,\omega_2)\tilde{u}^m(\mathbf{p}_3,\omega_3)\,, \tag{3.11}$$

and one 4-point vertex

$$J_{\rm int}^{4} = -\prod_{i=1}^{4}\int_{\mathbf{p}_i,\omega_i}\delta(\sum_{i=1}^{4}\mathbf{p}_i)\delta(\sum_{i=1}^{3}\omega_i)L_0p_1^a\left[\mu_0\delta^{\alpha\delta}\delta^{\beta\gamma}+\frac{\lambda_0}{2}\delta^{\alpha\beta}\delta^{\gamma\delta}\right](\mathbf{p}_1\cdot\mathbf{p}_2)(\mathbf{p}_3\cdot\mathbf{p}_4) \tag{3.12}$$
$$\times\tilde{h}^\alpha(\mathbf{p}_1,\omega_1)h^\beta(\mathbf{p}_2,\omega_2)h^\gamma(\mathbf{p}_3,\omega_3)h^\delta(\mathbf{p}_4,\omega_4).$$

Note that all legs of the vertices have a momentum factor. The diagramatic representation of the vertices is shown in figure 2.

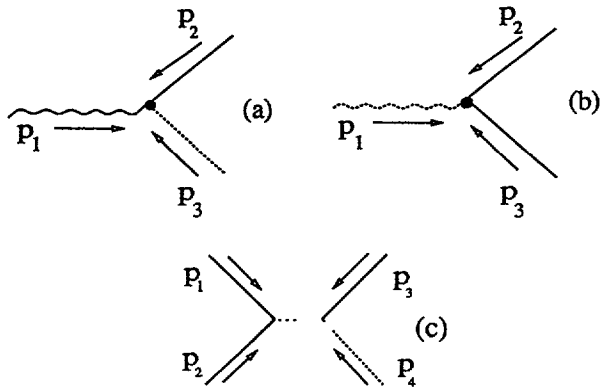

Fig. 2. — Interaction vertices in the dynamic functional. A wavy line corresponds to a phonon correlation field and a straight line to a undulation correlation field. The response fields are indicated by broken lines ((a): $J_{\rm int}^{3a}$, (b): $J_{\rm int}^{3b}$, (c): $J_{\rm int}^{4}$).

Since fluctuation-dissipation theorems play an important role in relating static and dynamic critical exponents, we study them next. Adding to the Hamiltonian "external" fields $B_{\rm h}$ and $B_{\rm u}$ which couple linearly to the undulation and phonon modes, the susceptibilities for the undulation modes,

$$\chi_{\rm h}^{\alpha\beta} = \frac{\delta < h^\alpha >}{\delta B_{\rm h}^\beta}|_{B_{\rm h}\to 0}\,, \tag{3.13}$$

and the phonon modes

$$\chi_{\rm u}^{ij} = \frac{\delta < u^i >}{\delta B_{\rm u}^j}|_{B_{\rm u}\to 0}, \tag{3.14}$$

can be written as [38]

$$\chi_{\rm h}^{\alpha\beta}(t) = -\Theta(t)\frac{\rm d}{{\rm d}t} < h^{\alpha}(t)h^{\beta}(0) > , \tag{3.15}$$

and

$$\chi_{\rm u}^{ij}(t) = -\Theta(t)\frac{\rm d}{{\rm d}t} < u^{i}(t)u^{j}(0) > . \tag{3.16}$$

On the other hand one finds directly from the dynamical functional (3.2-3.12) that

$$\chi_{\rm h}^{\alpha\beta}({\bf p},t) =< h^{\alpha}({\bf p},t)L_0 p^a \tilde{h}^{\beta}(-{\bf p},0) > , \tag{3.17}$$

$$\chi_{\rm u}^{ij}({\bf p},t) =< u^{i}({\bf p},t)D_{jl}^{0}({\bf p})\tilde{u}^{l}(-{\bf p},0) > . \tag{3.18}$$

This implies the following relations,

$$-i\omega\Gamma_{2000}^{0}({\bf p},\omega) = L_0 p^a \left(\Gamma_{1100}^{0}({\bf p},\omega) - \Gamma_{1100}^{0}(-{\bf p},-\omega)\right) , \tag{3.19}$$

$$-i\omega\Gamma_{0020}^{({\rm L,T})\,0}({\bf p},\omega) = D_0^{({\rm L,T})} p^a \left(\Gamma_{0011}^{({\rm L,T})\,0}({\bf p},\omega) - \Gamma_{0011}^{({\rm L,T})\,0}(-{\bf p},-\omega)\right) , \tag{3.20}$$

connecting different vertex functions. Here $\Gamma_{\tilde{M},M,\tilde{N},N}$ denotes a vertex function with $\tilde{M}$ undulation response fields $\tilde{h}$, M undulation correlation fields h, $\tilde{N}$ phonon response fields $\tilde{u}$, and N phonon correlation fields u. We shall now study the dynamic functional (3.2-3.12) using field-theoretic renormalization theory [38]. To remove the divergences, we introduce renormalization factors, which we choose to parameterize as follows:
(i) wave-function renormalization

$$u_{\rm R}^{i} = Z^{-1}u^{i} , \quad h_{\rm R}^{\alpha} = Z^{-1/2}h^{\alpha} , \quad \tilde{u}_{\rm R}^{i} = \tilde{Z}^{-1}\tilde{u}^{i} , \quad \tilde{h}_{\rm R}^{\alpha} = \tilde{Z}^{-1/2}\tilde{h}^{\alpha} , \tag{3.21}$$

(ii) kinetič coefficient renormalization

$$L_R = \tilde{Z}Z_{\rm L}^{-1}L_0 , \quad D_{\rm R}^{({\rm L,T})} = \tilde{Z}^2 Z_{\rm D}^{-1} D_0^{({\rm L,T})} , \tag{3.22}$$

(iii) and vertex renormalization

$$\mu_{\rm R} = M^{-\epsilon}Z^2 Z_{\mu}^{-1}\mu_0 , \quad \lambda_{\rm R} = M^{-\epsilon}Z^2 Z_{\lambda}^{-1}\lambda_0 , \tag{3.23}$$

where M is a reference wave number.

Due to the Ward identities [10] associated with the linearized rotational symmetry of the free energy functional $\mathcal{H}$, it is not necessary to introduce additional renormalization factors for the vertices, equations (3.10-3.12). Since the dynamics obeys detailed balance the renormalization factors Z, Z_λ, and Z_μ are the same as in statics [10]. The only renormalization factors left are those for the Onsager coefficients L_0 and $D_0^{({\rm L,T})}$. Using the structure of the vertices and the above fluctuation disspation theorems we will show next that these are not renormalized.

Since due to the wave vector dependence of the vertices all two point functions vanish in the limit $q \to 0$, one finds for the renormalized vertex functions

$$\partial_\omega \Gamma_{1100}({\bf q}=0) = i(Z\tilde{Z})^{1/2} \tag{3.24}$$

and

$$\partial_\omega \Gamma_{0011}(\mathbf{q}=0) = i(Z\tilde{Z})\,. \tag{3.25}$$

This implies the relation

$$Z\tilde{Z} = 1 \tag{3.26}$$

between the Z-factors for the field renormalization of the response and correlation fields, which is exact to all orders in perturbation theory.

Inserting in the fluctuation-dissipation theorem (3.19) the definitions (3.21-3.23) one finds for the renormalized vertex functions of the undulation modes

$$-i\omega\tilde{Z}^{-1}\Gamma_{2000}(\mathbf{p},\omega) = \tilde{Z}^{-1}Z_L L_R (Z\tilde{Z})^{-1/2} p^a \left(\Gamma_{1100}(\mathbf{p},\omega) - \Gamma_{1100}(-\mathbf{p},-\omega)\right)\,. \tag{3.27}$$

Therefore there is the following exact identity

$$\tilde{Z}^{-1} = Z_L \tilde{Z}^{-1}(Z\tilde{Z})^{-1/2}\,, \tag{3.28}$$

relating the renormalization factors of the fields and the kinetic coefficient of the undulation mode. With equation (3.26) we find

$$Z_L = 1\,, \tag{3.29}$$

i.e., there is no renormalization of the kinetic coefficient of the undulation modes. For the phonon modes one finds analogously

$$\tilde{Z}^{-2} = Z_D \tilde{Z}^{-2}(Z\tilde{Z})^{-1}\,, \tag{3.30}$$

and with (3.26)

$$Z_D = 1\,. \tag{3.31}$$

This implies that there is no dynamic renormalization of the Onsager coefficients for the undulation and phonon modes. All exponents including the dynamic critical exponents are therefore solely determined by the static renormalization factors and fixed points. Therefore the typical linewidth for the phonon modes Γ_u and for the undulation modes Γ_h have the following wave vector dependences

$$\Gamma_u \sim p^{a+2+\omega}\,, \tag{3.32}$$

$$\Gamma_h \sim p^{a+D+2\zeta}\,, \tag{3.33}$$

implying that the dynamic critical exponents are $z_h = a + D + 2\zeta$ and $z_u = a + 2 + \omega$, as quoted in the Introduction for $D = 2$ and $d = 3$.

Knowing the critical exponents there are two possible ways of calculating the scaling functions. One is to calculate the non divergent parts of the vertex functions in an ϵ-expansion. Here we use a second approach, which is analogous to mode coupling theory, namely to sum up the most divergent diagrams in the perturbation series and take into account the statics by using the fully renormalized static susceptibilities [42].

The resulting set of self consistent equations (see the Appendix) lead to the following scaling behavior of the correlation $C(\mathbf{p},\omega)$ and response functions $R(\mathbf{p},\omega)$

$$C_{\rm h}(p,\omega) = \frac{L_h p^a}{(L_h \kappa p^{a+2+2\zeta})^2} \hat{C}_{\rm h}(\hat{\omega}) \tag{3.34a}$$

$$R_{\rm h(p,\omega)} = \frac{1}{L_h \kappa p^{a+2+2\zeta}} \hat{R}_{\rm h}(\hat{\omega}) , \tag{3.34b}$$

$$C_{\rm u}^{\rm L,T}(p,\omega) = \frac{D^{\rm L,T} p^{a+\omega-2\zeta}}{(D^{\rm L,T} p^a \chi^{L,T}(p))^2} \hat{C}_{\rm u}^{L,T}(\hat{\omega}) , \tag{3.35a}$$

$$R_{\rm u}^{\rm L,T}(p,\omega) = \frac{1}{D^{\rm L,T} p^a \chi^{L,T}(p)} \hat{R}_{\rm u}^{\rm L,T}(\hat{\omega}) , \tag{3.35b}$$

where $\hat{C}$ and $\hat{R}$ are scaling functions and we have specialized to $D = 2$ and $d = 3$. $L_{\rm h}$ denotes the renormalized kinetic coefficient for the undulation modes. The scaling variable for the frequency is given by

$$\hat{\omega} = \frac{\omega}{L_{\rm h} \kappa p^{a+2+2\zeta}} , \tag{3.36}$$

i.e., it is characterized by the linewidth of the slowest mode, namely the undulation modes. With this scaling Ansatz all diagrams contributing to the vertex functions of the undulation modes have the same wave vector dependence. The frequency dependence of the vertex function Γ_{11} for the phonon modes has a subleading frequency dependence. This can be explicitly seen from the scaling form

$$\Gamma_{11}^{lm}(p,\omega)|_{\rm phonon} = D^{\rm T} \mu p^{a+2+\omega} \left[-i\hat{\omega} \frac{L_{\rm h} \kappa}{D^{\rm T} \mu} p^{2\zeta-\omega} + D^{lm}(\hat{\omega}) \right] , \tag{3.37}$$

where the first term in the square brackets is the subleading frequency dependence. The leading frequency dependence comes from the mode coupling contribution D^{lm} representing the decay of phonon modes into undulation modes (see Eq. (A.33)). Hence there are two time scales for the decay of the phonon modes. There is an initial decay due to the internal phonon dynamics and there is a much slower second decay due to the coupling to the out-of-plane modes.

One should further note that the anomalous scaling of the correlation function of the phonon modes (the term $D^{\rm L,T} p^{a+\omega-2\zeta}$) is a consequence of the fact that the scaling of the frequency variable is determined by the line width of the undulation modes. This is not a renormalization of the kinetic coefficients $D^{\rm L,T}$, as can be seen from the scaling of the response function (note that there is a fluctuation-dissipation relation: $i\omega\Gamma_{20}^{\rm L,T}(\omega) = D^{\rm L,T}[\Gamma_{11}^{\rm L,T}(\omega) - \Gamma_{11}^{\rm L,T}(-\omega)]$).

The structure of the correlation function for the undulation modes is mainly determined by the first mode coupling contribution, which is frequency independent. The phonon-mediated mode coupling terms vanish in the limit $\omega \to 0$. Hence to a first approximation , the shape of the correlation function is given by a Lorentzian, where the line width is given by the wave vector dependence of the bending rigidity. For more information on the scaling function one has to solve the equations discussed in the Appendix with a self consistent numerical procedure.

4. Dynamic structure factor.

The structure factor $S(\vec{k},t)$ observed in dynamic light scattering or neutron scattering experiments is given by the Fourier transform of the density-density correlation function

$$S(\vec{k},t) = \frac{1}{\mathcal{N}} \int \mathrm{d}^D s \int \mathrm{d}^D s' G(\vec{k},t;\mathbf{s},\mathbf{s}') , \tag{4.1}$$

where

$$G(\vec{k},t;\mathbf{s},\mathbf{s}') = < \exp\left[i\vec{k}\cdot\left(\vec{R}(\mathbf{s},t) - \vec{R}(\mathbf{s}',0)\right)\right] > = \mathrm{e}^{i\mathbf{k}_\perp\cdot(\mathbf{s}-\mathbf{s}')} g(\vec{k},t;\mathbf{s},\mathbf{s}') . \tag{4.2}$$

Here $\mathbf{k}_\perp$ is the in-plane part of $\vec{k}$ and $\mathcal{N}$ is determined by the normalization $S(\vec{k}=0,t=0)=1$.

The behavior of the dynamic structure factor has two limiting regimes depending on whether the wave length is much larger or much smaller than the linear dimension L of the membrane. In the regime $k_\perp mL << 1$, where the wave length is much larger than the linear dimension of the membrane, only the overall translational (and rotational) motion of the membrane can be seen in the dynamic structure function. Hence the dynamic scattering function in the long time limit is given by

$$S(\vec{k},t) = \exp\left[-\mathcal{D}k^2 t\right] , \tag{4.3}$$

where the diffusion constant $\mathcal{D}$ for the center of mass motion can be calculated with the Kirkwood formula [44,45], which is simply the Oseen tensor in the Markovian approximation at zero wave vector. In the case of a disc geometry the diffusion constant is

$$\mathcal{D} = \frac{k_\mathrm{B}T}{6\pi\eta}\left(\frac{4}{\pi L^2}\right)^2 \int_{|\mathbf{s}|<L/2} \mathrm{d}^2 s \int_{|\mathbf{s}'|<L/2} \mathrm{d}^2 s' \left\langle \frac{1}{|\vec{R}(\mathbf{s},t) - \vec{R}(\mathbf{s}',t)|} \right\rangle . \tag{4.4}$$

For a rigid disc (i.e., $\vec{R} = (s_1, s_2, 0)$) this gives

$$\mathcal{D}_{\text{rigid disc}} \approx \frac{2k_\mathrm{B}T}{3\pi\eta L} \sim \frac{1}{L} . \tag{4.5}$$

In a factorization (mode coupling) approximation due to Kirkwood and Riseman [27,45] (equivalent to the preaveraging of the Oseen tensor with the linearized static functional with fully renormalized bending rigidity and Lamé coefficients) equation (4.4) reduces to

$$\mathcal{D} = \frac{k_\mathrm{B}T}{6\pi\eta} \int \mathrm{d}^d k S(\vec{k}) \frac{1}{k^2} , \tag{4.6}$$

where $S(\vec{k})$ is the normalized static structure factor, discussed in reference [15]. Using an effective, long wave length free energy functional with the fully renormalized elastic constants one finds

$$S(\vec{k}) = S(\mathbf{k}_\perp, k_z, L) = \left(\frac{4}{\pi L^D}\right)^2 \int_{|\mathbf{s}|<L/2} \mathrm{d}^D s \int_{|\mathbf{s}'|<L/2} \mathrm{d}^D s' \; F(\mathbf{s}-\mathbf{s}') , \tag{4.7}$$

where

$$F(\mathbf{s}) = \exp\left[i\mathbf{k}_\perp\cdot\mathbf{s} - \frac{1}{\kappa} k_z^2 A_h(\hat{e}_\mathbf{s})|\mathbf{s}|^{2\zeta} - k_\perp^i k_\perp^j \left(\frac{A_\mathrm{L}^{ij}(\hat{e}_\mathbf{s})}{\lambda+2\mu} + \frac{A_\mathrm{T}^{ij}(\hat{e}_\mathbf{s})}{\mu} \right) |\mathbf{s}|^{\omega+2-D} \right] \tag{4.8}$$

with the amplitudes $A_h(\hat{e}_s)$ and $A^{ij}_{L,T}(\hat{e}_s)$ given by equations (2.30,31). The wave vectors $\mathbf{k}_\perp$ and k_z denote the in-plane and out-of plane components of the scattering vector $\vec{k}$, respectively. The scaling analysis is completely analogous to the one we did for the preaveraged Oseen tensor in section 2.2. One finds for the molecular weight dependence of the diffusion constant in the flat phase

$$\mathcal{D}_{\text{flat}} \sim \frac{L^{-d_\infty+2}}{L^D} \tag{4.9}$$

corresponding to $\mathcal{D}_{\text{flat}} = L^{-1}$ in $d = 3$ dimensions for a $D = 2$ dimensional membrane. This is exactly the same result as for a rigid disc, equation (4.5). Note that for Rouse dynamics the diffusion constant would be

$$\mathcal{D}_{\text{Rouse}} = \frac{k_B T}{N^2 \zeta}, \tag{4.10}$$

where ζ is the friction coefficient of an individual bead and N is the number of monomers. This corresponds to a molecular weight dependence $\mathcal{D}_{\text{Rouse}} \sim L^{-2}$. Except for logarithmic corrections, equation (4.9), also contains the case of a rigid rod, where [24]

$$\mathcal{D}_{\text{rigid rod}} \sim \frac{\ln L}{L} \tag{4.11}$$

The above result for the flat phase has to be compared with what is obtained for the crumpled phase [23]

$$\mathcal{D}_{\text{crumpled}} \sim L^{-\nu(d-2)} \tag{4.12}$$

In $d = 3$ dimensions and taking the Flory value for the exponent $\nu = 4/5$ one obtains

$$\mathcal{D}_{\text{crumpled}} \sim L^{-4/5} \tag{4.13}$$

If the wave length is much smaller than the linear dimension of the membrane $k_\perp mL >> 1$ one is probing the internal motion of the membrane. This limit is equivalent to considering a membrane of infinite extent. Using again the Gaussian approximation for the dynamic free energy functional with fully renormalized coefficients one finds

$$\begin{aligned} g(\vec{k}, t; \mathbf{s}, \mathbf{s}') = \exp\left[-\frac{1}{2} k^i_\perp k^j_\perp < \left(u^i(\mathbf{s}, t) - u^i(\mathbf{s}', 0)\right)\left(u^j(\mathbf{s}, t) - u^j(\mathbf{s}', 0)\right) >\right] \\ \times \exp\left[-\frac{1}{2} k^2_\parallel < \left(h(\mathbf{s}, t) - h(\mathbf{s}', 0)\right)^2 >\right]. \end{aligned} \tag{4.14}$$

The correlation functions for the undulation modes and the phonon modes can be written as

$$\begin{aligned} C_h(\mathbf{s}, \mathbf{s}', t) &= < \left(h(\mathbf{s}, t) - h(\mathbf{s}', 0)\right)^2 > \\ &= \int_{\mathbf{p}} \left[2\chi_h(\mathbf{p})(1 - \cos(\mathbf{p} \cdot (\mathbf{s} - \mathbf{s}'))) + 2\chi_h(\mathbf{p}) \cos(\mathbf{p} \cdot (\mathbf{s} - \mathbf{s}'))\left(1 - e^{-\Gamma_h(\mathbf{p})t}\right)\right], \end{aligned} \tag{4.15}$$

and

$$C_{\mathrm{u}}^{ij}(\mathbf{s},\mathbf{s}',t) = < \left(u^i(\mathbf{s},t) - u^i(\mathbf{s}',0)\right)\left(u^j(\mathbf{s},t) - u^j(\mathbf{s}',0)\right) >$$
$$= \int_{\mathbf{p}} \left[2\chi_{\mathrm{u}}^{ij}(\mathbf{p})(1-\cos(\mathbf{p}\cdot(\mathbf{s}-\mathbf{s}'))) + 2\chi_{\mathrm{u}}^{il}(\mathbf{p})\cos(\mathbf{p}\cdot(\mathbf{s}-\mathbf{s}'))\left(\delta_{lj} - \mathrm{e}^{-\Gamma_{\mathrm{u}}^{lj}(\mathbf{p})t}\right)\right], \tag{4.16}$$

where $\chi_{\mathrm{h}}(\mathbf{p})$ and $\chi_{\mathrm{u}}^{ij}(\mathbf{p})$ are the fully renormalized static susceptibilties. The line widths are given by

$$\Gamma_{\mathrm{h}}(\mathbf{p}) = \frac{L_{\mathrm{h}}(\mathbf{p})}{\chi_{\mathrm{h}}(\mathbf{p})} \tag{4.17}$$

and

$$\Gamma_{\mathrm{u}}^{ij}(\mathbf{p}) = D_{\mathrm{u}}^{il}(\mathbf{p})(\chi_{\mathrm{u}}^{-1})^{lj}(\mathbf{p}) \tag{4.18}$$

with the kinetic coefficients given by equations (3.1.a,b) with the bare quantities L_0 and $D_0^{\mathrm{L,T}}$ replaced by the full renormalized ones, L_{h} and $D_{\mathrm{L,T}}$. For $t = 0$ the above expressions reduce to the static structure factor, discussed in reference [15].

Now we turn to a scaling analysis of the dynamic structure factor. By substituting $y^{D+2\zeta+a} = L_{\mathrm{h}}\kappa p^{D+2\zeta+a}t$ and analogous expressions for the phonon modes, where the exponent $a = 0$ corresponds to Rouse behavior and $a = d_{\mathrm{co}} - 2$ to Zimm dynamics, the correlation function can be written as

$$C_{\mathrm{h}}(\mathbf{s},\mathbf{s}',t) = \frac{2}{\kappa}\left(A_{\mathrm{h}}(\hat{e}_{\mathbf{s}})|\mathbf{s}-\mathbf{s}'|^{2\zeta} + l_{\mathrm{h}}^{2\zeta} f_{\mathrm{h}}((\mathbf{s}-\mathbf{s}')/l_{\mathrm{h}})\right) \tag{4.19}$$

and

$$C_{\mathrm{u}}^{ij}(\mathbf{s},\mathbf{s}',t) = \frac{2}{(\lambda+2\mu)}\left(A_{\mathrm{L}}^{ij}(\hat{e}_{\mathbf{s}})|\mathbf{s}-\mathbf{s}'|^{\omega+2-D} + l_{\mathrm{L}}^{\omega+2-D} f_{\mathrm{L}}^{ij}((\mathbf{s}-\mathbf{s}')/l_{\mathrm{L}})\right)$$
$$+\frac{2}{\mu}\left(A_{\mathrm{T}}^{ij}(\hat{e}_{\mathbf{s}})|\mathbf{s}-\mathbf{s}'|^{\omega+2-D} + l_{\mathrm{T}}^{\omega+2-D} f_{\mathrm{T}}^{ij}((\mathbf{s}-\mathbf{s}')/l_{\mathrm{T}})\right). \tag{4.20}$$

Here we have defined the characteristic lengths

$$l_{\mathrm{h}} = (L_{\mathrm{h}}\kappa t)^{1/(D+2\zeta+a)}, \tag{4.21}$$

$$l_{\mathrm{L}} = (D_{\mathrm{L}}(\lambda+2\mu)t)^{1/(2+\omega+a)}, \tag{4.22}$$

$$l_{\mathrm{T}} = (D_{\mathrm{T}}\mu t)^{1/(2+\omega+a)} \tag{4.23}$$

The scaling functions f_{h} and f_{u} are given by

$$f_{\mathrm{h}}(\mathbf{x}) = \int \mathrm{d}^D y \cos(\mathbf{x}\cdot\mathbf{y}) y^{-D-2\zeta}\left(1 - \mathrm{e}^{-y^{D+2\zeta+a}}\right) \tag{4.24}$$

and

$$f_{\mathrm{L,T}}^{ij}(\mathbf{x}) = \int \mathrm{d}^D y \cos(\mathbf{x}\cdot\mathbf{y}) y^{-2-\omega}\left(1 - \mathrm{e}^{-y^{2+\omega+a}}\right) P_{\mathrm{L,T}}^{ij}(\mathbf{y}). \tag{4.25}$$

The general case is rather complex. But, to extract the characteristic features of the dynamic behavior it is enlightening to study the two limits, where the scattering vector lies parallel and perpendicular to the membrane plane.

(i) For $k_\perp = 0$ the dynamic structure factor simplifies to the scaling form

$$S(\mathbf{k}_\perp = 0, k_\parallel, t) \sim k_\parallel^{-D/\zeta} \int \mathrm{d}^D x \exp\left(\frac{1}{\kappa}\left[-A_{\mathrm{h}}(\hat{e}_x)x^{2\zeta} - k_\parallel^2 (L_{\mathrm{h}}\kappa t)^{2\zeta/(D+2\zeta+a)} f_{\mathrm{h}}(\mathbf{x}/\rho)\right]\right), \tag{4.26}$$

where the scaling variable ρ is defined by

$$\rho = \left(k_\parallel^2 (L_{\mathrm{h}}\kappa t)^{2\zeta/(D+2\zeta+a)}\right)^{1/2\zeta} \tag{4.27}$$

In the long time limt $\rho >> 1$ the scaling function reduces to a constant

$$f(0) = \int \mathrm{d}^D y \left(1 - \mathrm{e}^{-y^{D+2\zeta+a}}\right) y^{-D-2\zeta} \tag{4.28}$$

independent of x. Hence in this regime the dynamic structure factor is given by a stretched exponential

$$S(\mathbf{k}_\perp = 0, k_\parallel, t) = S(\mathbf{k}_\perp = 0, k_\parallel, 0) \exp\left[-C_{\mathrm{h}} k_\parallel^2 t^\alpha\right], \tag{4.29}$$

where C_{h} is a constant given by (note $k_{\mathrm{B}}T$ is set equal to 1)

$$C_{\mathrm{h}} = \frac{1}{\kappa}(L_{\mathrm{h}}\kappa)^{2\zeta/(D+2\zeta+a)} f(0). \tag{4.30}$$

The stretching exponent

$$\frac{\alpha = 2\zeta}{D + 2\zeta + a} \tag{4.31}$$

is listed in table I for a set of values for the roughness exponent ζ (for $D = 2$ and $d = 3$).

Table I. — *Stretching exponents α and β for a set of theoretical and numerical values of the exponents ω and ζ for Rouse ($a = 0$) and Zimm ($a = -1$) dynamics ($D = 2$, $d = 3$). The case $(\omega, \zeta) = (0, 1)$ corresponds to a fluid membrane. $(\omega, \zeta) = (2/3, 2/3)$ is the result from a $1/d$-expansion to leading order* [7, 8, 10]. $(\omega, \zeta) = (0, 1/2)$ [39] *and* $(\omega, \zeta) = (0.2, 0.55)$ [40] *are results from numerical simulations of tethered membranes.*

	$\alpha\ (a = 0)$	$\beta\ (a = 0)$	$\alpha\ (a = -1)$	$\beta\ (a = -1)$
$\omega = 0, \zeta = 1$	$\frac{1}{2}$	0 *("ln")*	$\frac{2}{3}$	0 *("ln")*
$\omega = 0, \zeta = \frac{1}{2}$	$\frac{1}{3}$	0 *("ln")*	$\frac{1}{2}$	0 *("ln")*
$\omega = \frac{2}{3}, \zeta = \frac{2}{3}$	$\frac{2}{5}$	$\frac{1}{4}$	$\frac{4}{7}$	$\frac{2}{5}$
$\omega = 0.2, \zeta = 0.55$	$\frac{11}{31}$	$\frac{1}{11}$	$\frac{11}{21}$	$\frac{1}{6}$

(ii) For $k_{\|} = 0$ the dynamic structure factor is

$$S(\mathbf{k}_\perp, k_{\|} = 0, t) \sim k_\perp^{-D} \int \mathrm{d}^D x \mathrm{e}^{\mathrm{i}\mathbf{x}\cdot\hat{e}_\perp} \times$$
$$\times \exp\left(\frac{1}{\lambda + 2\mu}\left[-A_{\mathrm{L}}^{ij}(\hat{e}_s) k_\perp^{D-\omega} x^{\omega+2-D} - k_\perp^2 (D_{\mathrm{L}}(\lambda + 2\mu)t)^{(\omega+2-D)/(2+\omega+a)} f_{\mathrm{L}}^{ij}(\mathbf{x}/\rho_L)\right]\right) \times$$
$$\times \exp\left(\frac{1}{\mu}\left[-A_{\mathrm{T}}^{ij}(\hat{e}_s) k_\perp^{D-\omega} x^{\omega+2-D} - k_\perp^2 (D_{\mathrm{T}}\mu t)^{(\omega+2-D)/(2+\omega+a)} f_{\mathrm{T}}^{ij}(\mathbf{x}/\rho_T)\right]\right), \tag{4.32}$$

where $\hat{e}_\perp = \mathbf{k}_\perp/|\mathbf{k}_\perp|$ and the scaling variables are

$$\rho_{\mathrm{L}} = k_\perp (D_{\mathrm{L}}(\lambda + 2\mu)t)^{1/(2+\omega+a)}, \tag{4.33a}$$

$$\rho_{\mathrm{T}} = k_\perp (D_{\mathrm{T}}\mu t)^{1/(2+\omega+a)} \tag{4.33b}$$

For $\rho >> 1$ the scaling function reduces to a constant independent of x. Hence the dynamic structure factor is given by a stretched exponential

$$S(\mathbf{k}_\perp, k_{\|} = 0, t) \sim \exp\left[-C_{\mathrm{u}} k_\perp^2 t^\beta\right] \tag{4.34}$$

where C_{u} is a constant and the stretching exponent

$$\beta = \frac{\omega + 2 - D}{2 + \omega + a} \tag{4.35}$$

is listed in table I for a set of values for the exponent ω (for $D = 2$ and $d = 3$). The case $(\omega, \zeta) = (0, 1)$ corresponds to a fluid membrane. $(\omega, \zeta) = (2/3, 2/3)$ is the result from a $1/d$-expansion to leading order [7,8,10]. $(\omega, \zeta) = (0, 1/2)$ [30] and $(\omega, \zeta) = (0.2, 0.55)$ [40] are results from numerical simulations of tethered membranes. Since the exponent ω found in numerical simulations of tethered membranes is very small [30,40] this is an enormous stretching or equivalently, close to an algebraic decay.

For the crumpled phase one finds, using the results of reference [23], that the long time behavior of the dynamic structure factor is also given by an stretched exponential

$$S(k, t)_{\mathrm{crumpled}} \sim \exp\left[-C_c k^2 t^\gamma\right] \tag{4.36a}$$

with the stretching exponent

$$\gamma = \frac{2\nu}{2 + 2\nu - [D + \nu(2 - d)]}. \tag{4.36b}$$

Here ν is the exponent of the radius of gyration ($R_g \sim L^\nu$) and $D + \nu(2 - d)$ is the exponent of the preaveraged Oseen tensor. Taking the Flory value for the exponent $\nu = \dfrac{D+2}{d+2}$, one finds $\gamma = \dfrac{2}{3}$.

Now we consider (for $(D, d) = (2, 3)$) the special case that the phonon modes are not renormalized by the coupling to the undulation modes, i.e., $\omega = 0$. This case is interesting first because there is a static crossover from $(\zeta, \omega) = (1, 0)$ to the asymptotic values and second because it is not

yet clear from numerical simulations whether the exponent ω is close to or identically zero. Furthermore, it may be difficult to distinguish between these two cases experimentally. For in-plane scattering vectors the density-density correlation function is

$$G(\mathbf{k}_\perp, k_z = 0, t; \mathbf{s}, \mathbf{s}') = < \exp\left[i\vec{k} \cdot \left(\vec{R}(\mathbf{s}, t) - \vec{R}(\mathbf{s}', 0)\right)\right] > = \mathrm{e}^{i\mathbf{k}_\perp \cdot (\mathbf{s}-\mathbf{s}')} g(\mathbf{k}_\perp, k_z = 0, t; \mathbf{s}, \mathbf{s}') \,. \tag{4.37}$$

The angular average of g is of the form

$$g_{\mathrm{av}}(\mathbf{k}_\perp, k_z = 0, t; \mathbf{s}, \mathbf{s}') = \exp\left(k_\perp^2 \frac{k_\mathrm{B}T}{4\pi}\left[\frac{1}{\lambda + 2\mu}\int \frac{\mathrm{d}p}{p}(1 - J_0(p|\mathbf{s} - \mathbf{s}'|)\mathrm{e}^{-\Gamma_\mathrm{L}(p)t}) + \frac{1}{\mu}\int \frac{\mathrm{d}p}{p}(1 - J_0(p|\mathbf{s} - \mathbf{s}'|)\mathrm{e}^{-\Gamma_\mathrm{T}(p)t})\right]\right), \tag{4.38}$$

where J_0 is a Bessel function of the first kind. The line width for the phonon modes are

$$\Gamma_\mathrm{L}(p) = (\lambda + 2\mu) D_\mathrm{L} p^{2+a} \,, \tag{4.39a}$$

$$\Gamma_\mathrm{T}(p) = \mu D_\mathrm{T} p^{2+a} \,, \tag{4.39b}$$

where the exponent $a = 0$ for Rouse and $a = -1$ for Zimm dynamics. Note here $k_\mathrm{B}T$ is not set equal to 1 as elsewhere in this paper.

One should note that equation (4.38) is exactly the expression for the dynamic density-density correlation function of a two dimensional solid. For the static case ($t = 0$) one finds an algebraic decay [46]

$$g_{\mathrm{av}}(\mathbf{k}_\perp, k_z = 0, t = 0; \mathbf{s}, \mathbf{s}') = |\mathbf{s} - \mathbf{s}'|^{-\eta(T)} \tag{4.40}$$

with a temperature dependent exponent

$$\eta(T) = \frac{k_\perp^2 k_\mathrm{B}T(3\mu + \lambda)}{4\pi\mu(2\mu + \lambda)} \tag{4.41}$$

This power law decay leads to a power law singularity in $S(\mathbf{k}_\perp)$ at the reciprocal lattice points $\{\vec{G}\}$. For $\mathbf{k}_\perp \approx \vec{G}$, one gets

$$S(\mathbf{k}_\perp) \sim \frac{1}{|\mathbf{k}_\perp - \vec{G}|^{2-\eta(T)}} \tag{4.42}$$

The time dependence of the dynamic density-density correlation function is also given by an algebraic decay. The value of the exponent depends on the exponent of the kinetic coefficient, i.e., on a. One finds for large times

$$g_{\mathrm{av}}(\mathbf{k}_\perp, k_z = 0, t; \mathbf{s}, \mathbf{s}') = t^{-\eta(T)/A} \,, \tag{4.43}$$

where

$$A = \int_0^\infty \mathrm{d}y \, y^{1+a} \mathrm{e}^{-y^{2+a}} = \begin{cases} \frac{1}{2} & \text{for Rouse dynamics } (a = 0), \\ 1 & \text{for Zimm dynamics } (a = -1). \end{cases} \tag{4.44}$$

Hence the time decay is half as fast as the spatial decay for Rouse dynamics, but equally fast for Zimm dynamics. More generally, the density-density correlation function for the phonon modes has the scaling form

$$g_{\rm av}(\mathbf{k}_\perp, k_z = 0, t; \mathbf{s}, \mathbf{s}') = |\mathbf{s} - \mathbf{s}'|^{-\eta(T)} \hat{g}(|\mathbf{s} - \mathbf{s}'|/t^A) . \tag{4.45}$$

5. Flicker phenomenon in red blood cells.

The membrane of a erythrocyte or red blood cell is a thin material, only about 5 nm thick, and essentially lamellar in structure. It consists of a lipid bilayer (believed to be in a liquid phase) in which macromolecules are incorporated. In addition there is also a spectrin polymer network attached to the inner layer through proteins. The presence of the spectrin implies that unlike the phospholipid component of a biological membrane, the composite red blood cell membrane exhibits a shear modulus [47,48].

The shape of the cell is biconcave-discoid (of dimension $\sim 8\mu \times 2\mu$) under normal physiological conditions. In this state the membrane surface tension is very small and the red blood cells show a remarkable flicker phenomenon, which can be seen by phase contrast microscopy [28]. This flicker is a purely physical effect and due to thermal fluctuations of the cell thickness. It was first observed by Browicz [49] using ordinary light microscopy. More recently Brochard and Lennon [28] have measured the frequency spectrum for the flicker intensity (flicker spectrum). They interpret the spectrum in terms of a linear theory considering an essentially incompressible fluid membrane with bending rigidity but no shear modulus, which is completely impermeable for solvent molecules.

Recently the spectrin skeleton of erythrocytes has been separated from their natural environment [18]. These isolated spectrin networks differ from the composite red blood cell both in the magnitude of their in-plane bulk modulus and in their permeability for solvent molecules. Whereas the permeability of the red blood cell is mainly determined by the flow through small protein channels [16-18], the isolated spectrin network has a mesh size ranging from 20 nm to 200 nm [18] which makes it highly permeable for solvent molecules. As discussed in the Introduction and in Section 2, the permeability of the membrane determines the location of the crossover from Rouse to Zimm dynamics. Hence, we expect qualitatively different behavior for spektrin skeletons as opposed to red blood cells as a consequence of their different permeability and elastic properties.

We simplify to a model of two membranes, whose conformations are described by surfaces $\vec{R}^{(1)}$ and $\vec{R}^{(2)}$, separated at a fixed average distance $d = |< \vec{R}^{(1)} - \vec{R}^{(2)} >|$ [28], as shown in figure 3. We assume that the membranes are infinite in extent and are therefore neglecting boundary effects. This restricts our analysis to wave lengths smaller than the cell diameter ($\approx 7.5\ \mu$m). For larger wave lengths the closed geometry of the cell has to be taken into account. The free energy functional of each membrane is taken to be that of a flat membrane with bending rigidity and internal shear elasticity due to the spectrin network.

This model of two dynamically interacting membranes is also a starting point for investigating the dynamics of semidilute membrane solutions, where the inter-membrane interaction becomes of importance. From the two-membrane model considered below one may infer how the interplay between inter- and intra-membrane interaction leads to a screening of the long range hydrodynamic interaction in semidilute solutions. One direction for further study would be the dynamics of lamellar phases of tethered membranes [50-52], which should have some similarity with the dynamics of smectics [53].

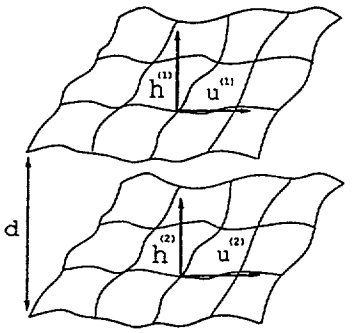

Fig. 3. — Model of two flat membranes separated at a distance d. The fluctuations of each membrane are characterized by bending $h^{(1,2)}$ and phonon modes $u^{(1,2)}$

In our model we neglect the static steric repulsion between the two membranes. Hence the interaction between the membranes is of purely dynamic origin and due to the backflow of the solvent fluid. The equations of motion for each membrane are then a straightforward generalization of equation (2.1),

$$\frac{\partial R_i^{(1,2)}(\mathrm{s},t)}{\partial t} = -L_{ij}\frac{\delta\mathcal{H}(\{\vec{R}^{(1,2)}\})}{\delta R_j^{(1,2)}(\mathrm{s},t)} + g v_i[\vec{R}^{(1,2)}(\mathrm{s},t),t] + \Theta_i^{(1,2)}(\mathrm{s},t)\,. \tag{5.1}$$

For notational convenience we omit all subscripts "0" indicating bare quantities in this section. The coupling between the membrane is mediated by the intervening solvent, whose velocity field obeys the following Langevin equation similar to equation (2.8),

$$\begin{aligned}\frac{\partial v_i(\vec{k},t)}{\partial t} + \nu k^2 v_i(\vec{k},t) = P_{ij}^{\mathrm{T}}(\hat{k})\Big[\zeta_j(\vec{k},t) &- \frac{g}{\rho}\int \mathrm{d}^D s \frac{\delta\mathcal{H}}{\delta R_j^{(1)}(\mathrm{s},t)}\exp\left(-i\vec{k}\cdot\vec{R}^{(1)}(\mathrm{s},t)\right)\\ &- \frac{g}{\rho}\int \mathrm{d}^D s \frac{\delta\mathcal{H}}{\delta R_j^{(2)}(\mathrm{s},t)}\exp\left(-i\vec{k}\cdot\vec{R}^{(2)}(\mathrm{s},t)\right)\Big]\,.\end{aligned} \tag{5.2}$$

Upon inserting the formal solution of the latter equation into the Langevin equation for the conformation fields of the membranes one finds, in the Markovian approximation for the solvent, the following coupled Langevin equations

$$\begin{aligned}&\frac{\partial R_i^{(1,2)}(\mathrm{s},t)}{\partial t} = -L_{ij}\frac{\delta\mathcal{H}(\{\vec{R}^{(1,2)}\})}{\delta R_j^{(1,2)}(\mathrm{s},t)} + \tilde{\Theta}_i^{(1,2)}(\mathrm{s},t)\\ &-g^2\int_k \frac{1}{\eta k^2}P_{ij}^{\mathrm{T}}(\hat{k})\int \mathrm{d}^D s' \frac{\delta\mathcal{H}}{\delta R^{(1,2)}(\mathrm{s}',t)}\exp\left[i\vec{k}\cdot\left(\vec{R}^{(1,2)}(\mathrm{s},t) - \vec{R}^{(1,2)}(\mathrm{s}',t)\right)\right]\\ &-g^2\int_k \frac{1}{\eta k^2}P_{ij}^{\mathrm{T}}(\hat{k})\int \mathrm{d}^D s' \frac{\delta\mathcal{H}}{\delta R^{(2,1)}(\mathrm{s}',t)}\exp\left[i\vec{k}\cdot\left(\vec{R}^{(1,2)}(\mathrm{s},t) - \vec{R}^{(2,1)}(\mathrm{s}',t)\right)\right]\end{aligned} \tag{5.3}$$

for the membrane conformations, where $\tilde{\Theta}_i^{(1,2)}(\mathrm{s},t)$ are noise terms modified similar as in section 2. Note that the equation of motion for each membrane contains two hydrodynamic interactions,

one is due to a intra-membrane and the other to a inter-membrane backflow. The interplay between these two effects will be of crucial importance for the dynamics of the thickness fluctuations (see below). In the preaveraging approximation, i.e., upon replacing $\vec{k}\cdot(\vec{R}^{(1)}(s)-\vec{R}^{(1)}(s'))$ by its average value $<\vec{k}\cdot(\vec{R}^{(1)}(s)-\vec{R}^{(1)}(s'))>=\mathbf{k}\cdot(s-s')$ and $\vec{k}\cdot(\vec{R}^{(1)}(s)-\vec{R}^{(2)}(s'))$ by its average value $<\vec{k}\cdot(\vec{R}^{(1)}(s)-\vec{R}^{(2)}(s'))>=\mathbf{k}\cdot(s-s')+ik_{\|}d$ (the in-plane wave vector is denoted by k), the equations of motion for the undulation and phonon modes of each membrane reduce to

$$\frac{\partial u_i^{(1)}(\mathbf{k},t)}{\partial t}=-D_{ij}^{\text{intra}}(\mathbf{k})\frac{\delta\mathcal{H}}{\delta u_j^{(1)}(-\mathbf{k},t)}-D_{ij}^{\text{inter}}(\mathbf{k})\frac{\delta\mathcal{H}}{\delta u_j^{(2)}(-\mathbf{k},t)}+i\frac{g^2d}{4\eta}\frac{k^i}{k}e^{-kd}\frac{\delta\mathcal{H}}{\delta h^{(2)}(-\mathbf{k},t)}+\tilde{\Theta}_i(\mathbf{k},t)\,, \tag{5.4a}$$

$$\frac{\partial u_i^{(2)}(\mathbf{k},t)}{\partial t}=-D_{ij}^{\text{intra}}(\mathbf{k})\frac{\delta\mathcal{H}}{\delta u_j^{(2)}(-\mathbf{k},t)}-D_{ij}^{\text{inter}}(\mathbf{k})\frac{\delta\mathcal{H}}{\delta u_j^{(1)}(-\mathbf{k},t)}-i\frac{g^2d}{4\eta}\frac{k^i}{k}e^{-kd}\frac{\delta\mathcal{H}}{\delta h^{(1)}(-\mathbf{k},t)}+\tilde{\Theta}_i(\mathbf{k},t)\,, \tag{5.4b}$$

$$\frac{\partial h^{(1)}(\mathbf{k},t)}{\partial t}=-L^{\text{intra}}(\mathbf{k})\frac{\delta\mathcal{H}}{\delta h^{(1)}(-\mathbf{k},t)}-L^{\text{inter}}(\mathbf{k})\frac{\delta\mathcal{H}}{\delta h^{(2)}(-\mathbf{k},t)}+i\frac{g^2d}{4\eta}\frac{k^j}{k}e^{-kd}\frac{\delta\mathcal{H}}{\delta u_j^{(2)}(-\mathbf{k},t)}+\tilde{\Theta}(\mathbf{k},t)\,, \tag{5.4c}$$

$$\frac{\partial h^{(2)}(\mathbf{k},t)}{\partial t}=-L^{\text{intra}}(\mathbf{k})\frac{\delta\mathcal{H}}{\delta h^{(2)}(-\mathbf{k},t)}-L^{\text{inter}}(\mathbf{k})\frac{\delta\mathcal{H}}{\delta h^{(1)}(-\mathbf{k},t)}-i\frac{g^2d}{4\eta}\frac{k^j}{k}e^{-kd}\frac{\delta\mathcal{H}}{\delta u_j^{(1)}(-\mathbf{k},t)}+\tilde{\Theta}(\mathbf{k},t)\,. \tag{5.4d}$$

The kinetic coefficients for the inter- and intra-membrane interaction are given by

$$D_{ij}^{\text{intra}}(\mathbf{k})=D_u\delta^{ij}+\frac{g^2}{2\eta k}\left(\delta^{ij}-\frac{1}{2}\frac{k_ik_j}{k^2}\right)\,, \tag{5.5a}$$

$$D_{ij}^{\text{inter}}(\mathbf{k})=\frac{g^2}{2\eta k}\left(\delta^{ij}-\frac{1}{2}(1+kd)\frac{k_ik_j}{k^2}\right)e^{-kd}\,, \tag{5.5b}$$

for the phonon modes (for simplicity we have assumed $D_L=D_T=D_u$), and by

$$L^{\text{intra}}(\mathbf{k})=L_h+\frac{g^2}{4\eta k}\,, \tag{5.6a}$$

$$L^{\text{inter}}(\mathbf{k})=\frac{g^2}{4\eta k}(1+kd)e^{-kd}\,, \tag{5.6b}$$

for the undulation modes. The above equations show that there is an inter-membrane coupling between the longitudinal phonon modes and the undulation modes, whereas the transverse phonon modes couple neither to the longitudinal phonon modes nor to the undulation modes. This decoupling results from the incompressibility of the intervening fluid. Although the shear modulus of the spectrin skeleton does not directly modify the spectrum of the thickness fluctuations, the

crosslinking inherent in the spectrin skeleton is responsible for the solid-like behavior of the cell membrane and therefore for the very strongly renormalized bending rigidity [4]. The amplitude of the shear modulus and the other elastic constants determine the static crossover wave length from fluid- to solid-like behavior of the membrane [30] (see also the end of this section). For recent experiments which study how crosslinking the cytoskeleton affects membrane undulations see reference [54].

For the further analysis of the Langevin equations it is convenient to decompose the phonon field into its transverse and longitudinal components

$$u_i = P_{\mathrm{L}}^{ij} u_j + P_{\mathrm{T}}^{ij} u_j = \frac{k_i}{k} u_{\mathrm{L}} + u_{i,\mathrm{T}}\,, \tag{5.7}$$

and to introduce the center of mass and relative coordinates,

$$h^{(\pm)} = h^{(1)} \pm h^{(2)}\,, \tag{5.8a}$$

$$u_{\mathrm{L}}^{(\pm)} = u_{\mathrm{L}}^{(1)} \pm u_{\mathrm{L}}^{(2)}\,, \tag{5.8b}$$

$$u_{i,\mathrm{T}}^{(\pm)} = u_{i,\mathrm{T}}^{(1)} \pm u_{i,\mathrm{T}}^{(2)}\,, \tag{5.8c}$$

of the fields. The equations of motion take the form

$$\frac{\partial u_{i,\mathrm{T}}^{(\pm)}}{\partial t} = -\left(D_{\mathrm{T}}^{\mathrm{intra}} \pm D_{\mathrm{T}}^{\mathrm{inter}}\right) \mu(k) k^2 u_{i,\mathrm{T}}^{(\pm)} \tag{5.9}$$

for the transverse phonon fields, and

$$\frac{\partial u_{\mathrm{L}}^{(+)}}{\partial t} = -\left(D_{\mathrm{L}}^{\mathrm{intra}} + D_{\mathrm{L}}^{\mathrm{inter}}\right) [\lambda(k) + 2\mu(k)] k^2 u_{\mathrm{L}}^{(+)} - i \frac{g^2 d}{4\eta} \mathrm{e}^{-kd} \kappa(k) k^4 h^{(-)}\,, \tag{5.10a}$$

$$\frac{\partial h^{(-)}}{\partial t} = -\left(L^{\mathrm{intra}} - L^{\mathrm{inter}}\right) \kappa(k) k^4 h^{(-)} + i \frac{g^2 d}{4\eta} \mathrm{e}^{-kd} [\lambda(k) + 2\mu(k)] k^2 u_{\mathrm{L}}^{(+)} \tag{5.10b}$$

for the coupling between the sum of the longitudinal phonon fields and the difference of the undulation modes, and

$$\frac{\partial u_{\mathrm{L}}^{(-)}}{\partial t} = -\left(D_{\mathrm{L}}^{\mathrm{intra}} - D_{\mathrm{L}}^{\mathrm{inter}}\right) [\lambda(k) + 2\mu(k)] k^2 u_{\mathrm{L}}^{(-)} + i \frac{g^2 d}{4\eta} \mathrm{e}^{-kd} \kappa(k) k^4 h^{(-)} \tag{5.11a}$$

$$\frac{\partial h^{(+)}}{\partial t} = -\left(L^{\mathrm{intra}} + L^{\mathrm{inter}}\right) \kappa(k) k^4 h^{(+)} - i \frac{g^2 d}{4\eta} \mathrm{e}^{-kd} [\lambda(k) + 2\mu(k)] k^2 u_{\mathrm{L}}^{(-)} \tag{5.11b}$$

for the coupling between the difference of the longitudinal phonon modes and the sum of the undulation modes. Here we have taken the free energy functional to be quadratic in the fields and have taken into account some effects of the nonlinearities by using the fully renormalized bending rigidity $\kappa(k)$ and Lamé coefficients $\lambda(k)$ and $\mu(k)$. This is justified by the fact that the kinetic coefficients of the above model are not renormalized (see Sect. 3).

The longitudinal and transverse kinetic coefficients for the phonon modes are given by

$$D_{\mathrm{T}}^{\mathrm{intra}} = D_u + \frac{g^2}{2\eta k}\,, \tag{5.12a}$$

$$D_{\mathrm{L}}^{\mathrm{intra}} = D_{\mathrm{u}} + \frac{g^2}{4\eta k}, \tag{5.12b}$$

for the intra-membrane interaction, and

$$D_{\mathrm{T}}^{\mathrm{inter}} = \frac{g^2}{2\eta k} e^{-kd}, \tag{5.13a}$$

$$D_{\mathrm{L}}^{\mathrm{inter}} = \frac{g^2}{4\eta k} (1 - kd)\, e^{-kd}, \tag{5.13b}$$

for the inter-membrane interaction. The coefficients D_{u} and L_{h} are proportional to the permeability of the membrane. For red blood cells the permeability is very low and hence these constants can be set to zero. For isolated spectrin networks, however, these constants are much larger as a consequence of their large mesh size.

The transverse phonon modes are completely decoupled from the rest of the modes. The linewidths are given by

$$i\omega_{1,2}^{\mathrm{T}} = D_{\mathrm{u}}\mu(k)k^2 + \frac{\mu(k)k}{2\eta}\left(1 \pm \mathrm{e}^{-kd}\right), \tag{5.14}$$

where here and in the remainder of this section we have set $g = 1$.

There is, however, a coupling between the longitudinal phonon modes and the bending modes, mediated by the intervening solvent. In discussing the two sets of coupled equations, equations (5.10.a,b) and equations (5.11.a,b) it is convenient to introduce a scaling variable for the frequency by

$$\hat{\omega} = \frac{4\eta\omega}{\kappa(k)k^3}, \tag{5.15}$$

which measures the frequency in units of the line width of the undulation modes of a single membrane (Zimm behavior). Furthermore we introduce two scaling variables for the wave vector

$$x = kd, \tag{5.16a}$$

$$z_\alpha = \begin{cases} k/k_{\mathrm{h}} = 4\eta L_{\mathrm{h}} k & \text{for } \alpha = \mathrm{h} \\ k/k_{\mathrm{u}} = 4\eta D_{\mathrm{u}} k & \text{for } \alpha = \mathrm{u} \end{cases} \tag{5.16b}$$

and a quantity

$$y = \frac{\lambda(k) + 2\mu(k)}{\kappa(k)k^2}, \tag{5.16c}$$

characterizing the ratio of stretching to bending energy. For red blood cells this ratio is usually very large, even for the smallest experimentally accessible wave vectors, due to the very low compressibility of the bilayer [48]. In the case of an isolated spectrin network, however, this ratio may eventually become smaller or even be of the order of unity.

The equations (5.10.a,b) describe the coupling between the relative mode of the undulations (thickness fluctuations) and the center of mass mode of the longitudinal phonon modes. The linewidths are found to be

$$i\hat{\omega}_{1,2} = \frac{1}{2}(ay + b) \pm \frac{1}{2}\sqrt{(ay - b)^2 + 4x^2 y \mathrm{e}^{-2x}}, \tag{5.17}$$

where we have defined the sum

$$a = 1 + (1 - x)e^{-x} + z_u \tag{5.18a}$$

and the difference

$$b = 1 - (1 + x)e^{-x} + z_h \tag{5.18b}$$

of the intra- and inter-membrane kinetic coefficients of the longitudinal phonon modes and the undulation modes, respectively, in terms of the scaling variables. The normalized eigenvectors are

$$\vec{e}_{1,2} = \left(iu_{1,2}^{(+)}, h_{1,2}^{(-)}\right), \tag{5.19}$$

with

$$u_{1,2}^{(+)} = \frac{-xe^{-x}}{\sqrt{(xe^{-x})^2 + (-i\hat{\omega}_{1,2} + ay)^2}}, \tag{5.20a}$$

$$h_{1,2}^{(-)} = \frac{-i\hat{\omega}_{1,2} + ay}{\sqrt{(xe^{-x})^2 + (-i\hat{\omega}_{1,2} + ay)^2}}. \tag{5.20b}$$

The wave vector dependence of the linewidths depends on two length scales, the distance between the membranes d and the crossover wave vectors $k_{u,h}$. It also depends on the ratio y of stretching to bending energy.

If the membrane shows no in-plane stiffness for longitudinal phonons ($y = 0$) there is only a bending mode with the linewidth

$$i\hat{\omega}_2 = b = z_h + 1 - (1 + x)e^{-x} \tag{5.21}$$

In the limit of wave lengths much smaller than the distance d between the membranes ($kd >> 1$) equation (5.21) reduces to $i\omega_2 = \frac{\kappa(k)k^3}{4\eta}(1 + k/k_h)$. In this limit the membranes are decoupled and the dynamics correspond to those of a single isolated membrane with a crossover from Rouse to Zimm dynamics at k_h. For long wave lengths or small distances between the two membranes, $kd << 1$, the line width is given by $i\omega_2 = \frac{\kappa(k)k^3}{4\eta}(k/k_h + (kd)^2/2)$. In this regime the dominant wave vector dependence of the line width is the Rouse term $L_h\kappa(k)k^4$ unless the permeability of the membrane for solvent molecules is very small. Hence we have the following crossover scenario for isolated spectrin networks in the case of $y = 0$. For wave numbers $k > k_h = 1/4\eta L_h$ the dynamics is governed by Rouse behavior. Then there is a crossover to Zimm behavior, which would be the ultimate long wave length limit of the dynamics of a single membrane. But, in the present case of two hydrodynamically coupled membranes, there is a reentrant crossover to Rouse dynamics at $kd = 1$. This is due to a screening of the hydrodynamic interaction (the $1/k$-singularity of the inter- and intra-membrane interaction cancel). The width of the Zimm regime is given by $k_h > k > 1/d$. If the membrane has a high permeability such that $k_h < 1/d$ one has Rouse dynamics over the entire wave vector regime. On the other hand, if the membrane is essentially impermeable (like a lipid bilayer) the crossover is form Zimm dynamics $i\omega_2 = \frac{\kappa(k)k^3}{4\eta}$ for $kd >> 1$ to $i\omega_2 = \frac{\kappa(k)k^3}{8\eta}(kd)^2$ for $kd << 1$ corresponding to a kinetic coefficient proportional to k^2.

For membranes with a very high resistance to compressions ($y >> 1$), as is usually the case for red blood cells, the bending mode has the linewidth

$$i\hat{\omega}_h = b - \frac{x^2 e^{-2x}}{a} \tag{5.22}$$

and the linewidth for the phonon mode has the form

$$i\hat{\omega}_L = ay = (k/k_u + 1 + (1-x)e^{-x})y . \tag{5.23}$$

For $kd >> 1$, where the two membranes fluctuate independently, one finds $i\omega_h = \frac{\kappa(k)k^3}{4\eta}(1 + k/k_h)$ for the undulation mode and $i\omega_L = \frac{[\lambda(k) + 2\mu(k)]k}{4\eta}(1 + k/k_u)$ for the longitudinal phonon mode.

In the regime $kd << 1$, where the two membranes are strongly coupled by the hydrodynamic interaction, the resulting linewidths differ from the above case. For essentially impermeable membranes, $k/k_h << 1$ and $k/k_u << 1$, the line width of the thickness fluctuations is $i\omega_h = \frac{\kappa(k)k^3}{4\eta}\frac{(kd)^3}{6}$ and the phonon modes show Zimm behavior $i\omega_L = \frac{(\lambda(k) + 2\mu(k))k}{2\eta}$, which has an amplitude two times larger than for $kd >> 1$. The result for the thickness fluctuations for impermeable membranes with a large ratio of stretching to bending energy corresponds to the result found by Brochard and Lennon [28] provided one assumes a liquid-like roughness exponent $\zeta = 1$. However, for highly permeable membranes like the isolated spectrin network the dominating wave vector dependence for the undulation and the phonon modes are given by $i\omega_h = L_h\kappa(k)k^4$ and $i\omega_L = D_u[\lambda(k) + 2\mu(k)]k^2$ cooresponding to Rouse dynamics. Therefore we have the same crossover scenario for highly permeable membranes independent of the magnitude of y. One should note that the result for the kinetic coefficient of highly permeable and impermeable membranes differ drastically, namely by two powers in the wave vector.

The coupling between the sum of the bending modes and the difference of the longitudinal phonon modes is described by equations (5.11.a,b). The linewidths are found to be

$$i\hat{\omega}_{1,2} = \frac{1}{2}(ay + b) \pm \frac{1}{2}\sqrt{(ay - b)^2 + 4x^2 y e^{-2x}} , \tag{5.24}$$

where now

$$a = 1 - (1 - x)e^{-x} + z_u , \tag{5.25a}$$

and

$$b = 1 + (1 + x)e^{-x} + z_h . \tag{5.25b}$$

The corresponding normalized eigenvectors are given equations (5.19-20) with a and b given by equations (5.25).

For $y = 0$ there is only a bending mode with linewidth

$$i\hat{\omega}_h = b = k/k_h + 1 + (1 + x)e^{-x} \tag{5.26}$$

By passing from wave vectors $kd << 1$ to $kd >> 1$ the amplitude of the Zimm term merely changes its amplitude by a factor of 2. One finds $i\omega_h = \frac{\kappa(k)k^3}{4\eta}(1 + k/k_h)$ for $kd >> 1$ and

$i\omega_h = \frac{\kappa(k)k^3}{4\eta}(2 + k/k_h)$ for $kd << 1$. In both regimes the sum of the undulation modes shows a crossover from Rouse to Zimm behavior similar as for an isolated membrane. In particular, there is no cancellation of the hydrodynamic $1/k$-singularity in the kinetic coefficients. This has to be contrasted with the behavior of the thickness fluctuations (difference of the undulation modes) discussed above.

For $y >> 1$ the linewidth of the bending mode reduces to

$$i\hat{\omega}_h = b - \frac{x^2 e^{-2x}}{a} \tag{5.27}$$

and for the phonon mode we find

$$i\hat{\omega}_L = ay = (k/k_u + 1 - (1-x)e^{-x})y\,. \tag{5.28}$$

In the limit $kd >> 1$ one recovers the results of two independent membranes. For $kd << 1$ there is no change in the wave vector dependence of sum of the the bending mode but merely an enhancement of the amplitude of the Zimm term, $i\omega_h = \frac{\kappa(k)k^3}{4\eta}(2 + k/k_h - kk_u d/(2k_u d + 1))$. The relative longitudinal phonon mode has the line width $i\omega_L = \frac{[\lambda(k) + 2\mu(k)]k}{4\eta}(k/k_u + 2kd)$ corresponding to Rouse dynamics for both highly permeable and impermeable membranes.

In summary, we have found the following crossover scenario for the thermal thick ness fluctuations (flickering). The crossover in the line width depends sensitively on the permeability of the membrane.

For highly permeable membranes, like the isolated spectrin network, we find a crossover from Rouse to Zimm behavior at a wave vector $k_h = 1/4\eta L_h$. As a consequence of hydrodynamic screening effects there is a reentrant crossover to Rouse dynamics at $kd = 1$ with $L_{eff}(k \to 0) = L_h$. The Zimm behavior is restricted to a wave vector regime $1/4\eta L_h > k > 1/d$. For highly permeable membranes this becomes a very narrow regime or even vanishes if $k_h < 1/d$.

A completely different crossover scenario is obtained for impermeable membranes, like the composite red blood cell. There one has to distinguish between large and small ratio of stretching to bending energy y. For $y >> 1$, which is the case for red blood cells, one obtains a crossover from Zimm dynamics with a kinetic coefficient proportional to $L_{eff} \sim 1/k$ to a kinetic coefficient $L_{eff}(k \to 0) = k^2 d^3/24\eta$. In the regime $y << 1$ the linewidth shows a crossover from Zimm dynamics to $i\omega_h = \kappa(k)k^3(kd)^2/8\eta$ corresponding to a kinetic coefficient proportional to $L_{eff} \sim k$.

The crossover scenario of the fluctuations of the difference $[u^{(1)}(\mathbf{k},t) - u^{(2)}(\mathbf{k},t)]$ of the in-plane modes is similar to the scenario of the thickness fluctuations in the case of highly permeable membranes. The asymptotic behavior is Rouse-like with $D_{eff}^{L,T}(k \to 0) = D_u$. For impermeable membranes the crossover is from Zimm to Rouse dynamics with $D_{eff}^{L,T}(k \to 0) = d/2\eta$.

The correlation function for the thickness fluctuations is given by

$$C_d(k,\omega) = \frac{L_{eff}(k)}{\omega^2 + [\kappa(k)k^4 L_{eff}(k)]^2}\,, \tag{5.29}$$

where for $y >> 1$ the effective kinetic coefficient is given by

$$L_{eff}(k) = \frac{1}{4\eta k}\left[k/k_h + 1 - (1+kd)e^{-kd} - \frac{(kd)^2 e^{-2kd}}{k/k_u + 1 - (1-kd)e^{-kd}}\right]. \tag{5.30}$$

One should note that there are two types of crossovers, which determine the actual wave vector dependence of the line width. First, there is a dynamic crossover described above. But second,

there is also a superimposed static crossover associated with the wave vector dependence of the bending rigidity. For relatively large values of the amplitude of the bending rigidity or relatively small shear modulus, the small wave length modes of the membrane are characterized by fluid like behavior with a roughness exponent $\zeta = 1$. It is only for larger wave length when the systems shows a crossover to the true asymptotic behavior with ζ close to 1/2. The crossover length scale found from numerical simulations [30] is given by

$$l = \frac{2\pi\kappa}{c(T\Upsilon)^{1/2}} \tag{5.31}$$

with the Young modulus $\Upsilon = 4\mu(\lambda + \mu)/(2\mu + \lambda)$ and $c = 1.3$. Hence depending on the numerical values of the amplitudes of the elastic constants and the viscosities, these crossovers will be mixed up.

Next we consider the flicker spectrum

$$G(\omega) = \int \mathrm{d}^2 q C_d(q,\omega)\,. \tag{5.32}$$

Scaling gives the following power law for this quantity

$$G(\omega) \sim \omega^{-\sigma}\,, \tag{5.33}$$

with

$$\sigma = \frac{(2 + 4\zeta + b)}{(2 + 2\zeta + b)}\,, \tag{5.34}$$

where b is the exponent of the effective kinetic coefficient $L_{\mathrm{eff}}(k) \sim k^b$. The values of the exponent σ are summarized in table II for different values of the roughness exponent, corresponding to fluid like and solid like membranes.

Table II. — *Exponent σ of the frequency dependence of the flicker spectrum for a kinetic coefficient $L_{\mathrm{eff}} \sim k^b$ for different values of the roughness exponent* [7, 8, 10, 39, 40] *(see also Tab. I) corresponding to solid-like and fluid-like membranes.*

ζ	$b = 2$	$b = -1$ [Zimm]	$b = 0$ [Rouse]
1 *(fluid)*	$\frac{4}{3}$	$\frac{5}{3}$	$\frac{3}{2}$
$\frac{1}{2}$ *(solid)*	$\frac{6}{5}$	$\frac{3}{2}$	$\frac{4}{3}$
$\frac{2}{3}$ *(solid)*	$\frac{5}{4}$	$\frac{11}{7}$	$\frac{7}{5}$
0.55 *(solid)*	$\frac{62}{52}$	$\frac{32}{21}$	$\frac{42}{31}$

A first indication of the dynamic crossover has recently been observed experimentally [55]. Since the resulting exponents for the frequency spectrum $G(\omega)$ are not very sensitive to the actual value of the roughness exponent, rather precise experiments are necessary to distinguish between

fluid and solid-like behavior. An easier experiment might be the measurement of the frequency and wave vector dependent correlation function.

As we have shown above, the crossover scenario, upon passing from $kd << 1$ to $kd >> 1$, depends sensitively on two factors, the permeability and the ratio of stretching to bending energy. This becomes evident if one considers the two extremal cases (i) an impermeable fluid ($\zeta = 1$) lipid bilayer (with $y >> 1$) [28] and (ii) polymerized ($\zeta \approx 0.5$) isolated spectrin networks with high permeability. The line width for the flicker modes are $\Gamma_h^{(i)} \sim k^6$ and $\Gamma_h^{(ii)} \sim k^3$, respectively, i.e., they differ by three powers in the wave vector !

Furthermore, the in-plane modes show interesting behavior. These modes have up to now not been studied experimentally. It would therefore be interesting to to design experiments, which allow to measure the in-plane dynamics of the membrane.

Acknowledgements.

It is a pleasure to acknowledge helpful discussions with D. Branton, C.F. Schmidt and K. Svoboda. One of us (E.F.) acknowledges support from a grant from the Deutsche Forschungsgemeinschaft. This work was also supported by the National Science Foundation, through grant DMR 88-17291 and through the Harvard Materials Research Laboratory.

Appendix

Self consistent theory and scaling functions.

In formulating a self consistent theory we start with integrating out the phonon modes. This can be done since the in-plane degrees of freedom enter only quadratically in the dynamic functional. The effect of integrating out the phonon modes will be to introduce new effective interactions between the out-of-plane undulations mediated by the "exchange" of phonons.

Upon combining the harmonic part of the dynamic functional, equation (3.5), with the two 3-point vertices, equations (3.10-11), containing the phonon fields one can write the phonon part of the dynamic functional as

$$\begin{aligned} J_{\text{phonon}} = &- \frac{1}{2}\int_{\mathbf{p}}\int_{\omega}(\tilde{u}^i(\mathbf{p},\omega), u^i(\mathbf{p},\omega))\mathbf{A}_u^{ij}(\mathbf{p},\omega)(\tilde{u}^j(-\mathbf{p},-\omega), u^j(-\mathbf{p},-\omega))^{\mathrm{T}} \\ &+ \int_{\mathbf{p}}\int_{\omega}\left[\tilde{Q}^l(\mathbf{p},\omega)u^l(-\mathbf{p},-\omega) + Q^l(\mathbf{p},\omega)\tilde{u}^l(-\mathbf{p},-\omega)\right] . \end{aligned} \tag{A.1}$$

Here we have introduced the composite undulation operators

$$\tilde{Q}^l(\mathbf{p},\omega) = i\delta^{\alpha\beta}\prod_{i=1}^{2}\int_{\mathbf{p}_i}\int_{\omega_i}\delta(\mathbf{p}_1+\mathbf{p}_2+\mathbf{p})L_0 p_1^a V^l(\mathbf{p}_1,\mathbf{p}_2,\mathbf{p})\tilde{h}^\alpha(\mathbf{p}_1,\omega_1)h^\beta(\mathbf{p}_2,\omega_2)\,, \tag{A.2}$$

$$\begin{aligned} Q^l(\mathbf{p},\omega) = \frac{i}{2}\delta^{\alpha\beta}\prod_{i=1}^{2}\int_{\mathbf{p}_i}\int_{\omega_i}\delta(\mathbf{p}_1+\mathbf{p}_2+\mathbf{p})\Big[&D_0^{\mathrm{T}}p^a P_{lm}^{\mathrm{T}}(\mathbf{p})V^m(\mathbf{p}_1,\mathbf{p}_2,\mathbf{p}) \\ &+D_0^{\mathrm{L}}p^a P_{lm}^{\mathrm{L}}(\mathbf{p})V^m(\mathbf{p}_1,\mathbf{p}_2,\mathbf{p})\Big]h^\alpha(\mathbf{p}_1,\omega_1)h^\beta(\mathbf{p}_2,\omega_2)\,. \end{aligned} \tag{A.3}$$

The vertex factors are defined by (see Eqs. (3.10-11))

$$V^l(\mathbf{p}_1,\mathbf{p}_2,\mathbf{p}_3) = \mu_0\left[(\mathbf{p}_3\cdot\mathbf{p}_1)p_2^l + (\mathbf{p}_3\cdot\mathbf{p}_2)p_1^l\right] + \lambda_0(\mathbf{p}_1\cdot\mathbf{p}_2)p_3^l\,. \tag{A.4}$$

Since the phonon fields enter only linearly in the dynamic functional they can be integrated out by

$$J^{\rm eff}_{\rm phonon} = \int \mathcal{D}[i\tilde{u}]\int \mathcal{D}[u]J_{\rm phonon}\,, \tag{A.5}$$

resulting in new effective 4-point vertices,

$$J^{\rm eff}_{\rm phonon} = \frac{1}{2}\int_{\mathbf{p}}\int_{\omega}\left(Q^l(\mathbf{p},\omega),\tilde{Q}^l(\mathbf{p},\omega)\right)(\mathbf{A}_u^{-1})^{lm}(\mathbf{p},\omega)\left(Q^m(-\mathbf{p},-\omega),\tilde{Q}^m(-\mathbf{p},-\omega)\right)^{\rm T}\,, \tag{A.6}$$

describing the long-ranged phonon-mediated interaction between the undulation modes (for integrating out the phonon modes in statics see Refs. [1,4]). The "exchange" propagators are given by

$$(\mathbf{A}_u^{-1})^{ij}(\mathbf{p},\omega) = (\mathbf{A}_u^{-1})^{\rm T}(\mathbf{p},\omega)P_{ij}^{\rm T}(\mathbf{p}) + (\mathbf{A}_u^{-1})^{\rm L}(\mathbf{p},\omega)P_{ij}^{\rm L}(\mathbf{p})\,, \tag{A.7}$$

where

$$(\mathbf{A}_u^{-1})^{\rm T}(\mathbf{p},\omega) = \frac{1}{\omega^2 + [D_0^{\rm T}p^a\mu_0p^2]^2}\begin{pmatrix} 0 & i\omega + D_0^{\rm T}p^a\mu_0p^2 \\ -i\omega + D_0^{\rm T}p^a\mu_0p^2 & 2D_0^{\rm T}p^a\end{pmatrix}\,, \tag{A.8}$$

$$\begin{aligned}(\mathbf{A}_u^{-1})^{\rm L}(\mathbf{p},\omega) =& \frac{1}{\omega^2 + [D_0^{\rm L}p^a(\lambda_0+2\mu_0)p^2]^2} \\ &\times\begin{pmatrix} 0 & i\omega + D_0^{\rm L}p^a(\lambda_0+2\mu_0)p^2 \\ -i\omega + D_0^{\rm L}p^a(\lambda_0+2\mu_0)p^2 & 2D_0^{\rm L}p^a\end{pmatrix}\,.\end{aligned} \tag{A.9}$$

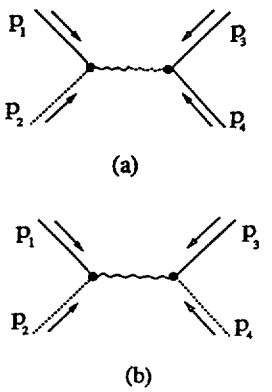

Fig. 4. — New effective phonon-mediated four-point vertices after integrating out the phonon modes ((a): $J^{4a}_{\rm eff}$, (b): $J^{4b}_{\rm eff}$).

More explicitly we find two new vertices, depicted in figure 4. The corresponding analytic expressions are

$$J^{4a}_{\rm eff} = -\frac{1}{2}\int_{\mathbf{p}}\int_{\mathbf{p}_1}\int_{\mathbf{p}_2}\int_{\omega}\int_{\omega_1}\int_{\omega_2} L_0 p_1^a v_a(\mathbf{p}_1,\mathbf{p},\mathbf{p}_2,\omega)\times \\ \times\tilde{h}^{\alpha}(\mathbf{p}_1,\omega_1)h^{\alpha}(\mathbf{p}-\mathbf{p}_1,\omega-\omega_1)h^{\beta}(\mathbf{p}_2,\omega_2)h^{\beta}(-\mathbf{p}-\mathbf{p}_2,-\omega-\omega_2)\,, \tag{A.10}$$

$$J^{4b}_{\rm eff} = -\frac{1}{2}\int_{\mathbf{p}}\int_{\mathbf{p}_1}\int_{\mathbf{p}_2}\int_{\omega}\int_{\omega_1}\int_{\omega_2} L_0 p_1^a L_0 p_2^a v_b(\mathbf{p}_1,\mathbf{p},\mathbf{p}_2,\omega) \\ \times\tilde{h}^{\alpha}(\mathbf{p}_1,\omega_1)h^{\alpha}(\mathbf{p}-\mathbf{p}_1,\omega-\omega_1)\tilde{h}^{\beta}(\mathbf{p}_2,\omega_2)h^{\beta}(-\mathbf{p}-\mathbf{p}_2,-\omega-\omega_2)\,, \tag{A.11}$$

where the vertices are given by

$$v_a(\mathbf{p}_1,\mathbf{p},\mathbf{p}_2,\omega) = V^l(\mathbf{p}_1,\mathbf{p}-\mathbf{p}_1,-\mathbf{p})\left[\frac{D_0^{\rm T}p^a P^{\rm T}_{lm}(\mathbf{p})}{i\omega + D_0^{\rm T}p^a\mu_0 p^2} + \frac{D_0^{\rm L}p^a P^{\rm L}_{lm}(\mathbf{p})}{i\omega + D_0^{\rm L}p^a(\lambda_0+2\mu_0)p^2}\right]V^m(\mathbf{p}_2,-\mathbf{p}-\mathbf{p}_2,\mathbf{p})\,, \tag{A.12}$$

$$v_b(\mathbf{p}_1,\mathbf{p},\mathbf{p}_2,\omega) = V^l(\mathbf{p}_1,\mathbf{p}-\mathbf{p}_1,-\mathbf{p})\left[\frac{2D_0^{\rm T}p^a P^{\rm T}_{lm}(\mathbf{p})}{\omega^2 + [D_0^{\rm T}p^a\mu_0 p^2]^2} + \frac{2D_0^{\rm L}p^a P^{\rm L}_{lm}(\mathbf{p})}{\omega^2 + [D_0^{\rm L}p^a(\lambda_0+2\mu_0)p^2]^2}\right]V^m(\mathbf{p}_2,-\mathbf{p}-\mathbf{p}_2,\mathbf{p})\,. \tag{A.13}$$

The vertices are frequency dependent indicating that there are retardation effects in the phonon-mediated interaction. The retardation time is proportional to the lifetime of the transverse and longitudinal phonons. The vertex $J^{4a}_{\rm eff}$ can be combined with the original 4-point vertex $J^a_{\rm int}$ to give

$$J^{4a\prime}_{\rm eff} = -\frac{1}{2}\int_{\mathbf{p}}\int_{\mathbf{p}_1}\int_{\mathbf{p}_2}\int_{\omega}\int_{\omega_1}\int_{\omega_2} L_0 p_1^a v'_a(\mathbf{p}_1,\mathbf{p},\mathbf{p}_2,\omega) \\ \times\tilde{h}^{\alpha}(\mathbf{p}_1,\omega_1)h^{\alpha}(\mathbf{p}-\mathbf{p}_1,\omega-\omega_1)h^{\beta}(\mathbf{p}_2,\omega_2)h^{\beta}(-\mathbf{p}-\mathbf{p}_2,-\omega-\omega_2)\,, \tag{A.14}$$

where

$$v'_a(\mathbf{p}_1,\mathbf{p},\mathbf{p}_2,\omega) = V^l(\mathbf{p}_1,\mathbf{p}-\mathbf{p}_1,-\mathbf{p})\left[P^{\rm T}_{lm}(\mathbf{p})\left(\frac{D_0^{\rm T}p^a}{i\omega + D_0^{\rm T}p^a\mu_0 p^2} - \frac{1}{\mu_0 p^2}\right) + P^{\rm L}_{lm}(\mathbf{p})\left(\frac{D_0^{\rm L}p^a}{i\omega + D_0^{\rm L}p^a(\lambda_0+2\mu_0)p^2} - \frac{1}{(\lambda_0+2\mu_0)p^2}\right)\right]V^m(\mathbf{p}_2,-\mathbf{p}-\mathbf{p}_2,\mathbf{p})\,, \tag{A.15}$$

and

$$J^{4\,\prime}_{\rm eff} = -\frac{1}{2}\int_{\mathbf{p}}\int_{\mathbf{p}_1}\int_{\mathbf{p}_2}\int_{\omega}\int_{\omega_1}\int_{\omega_2} L_0 p_1^a \frac{4\mu_0(\mu_0+\lambda_0)}{2\mu_0+\lambda_0}(p_1^{\alpha}P^{\rm T}_{\alpha\beta}(\mathbf{p})p_1^{\beta})(p_2^{\gamma}P^{\rm T}_{\gamma\delta}(\mathbf{p})p_2^{\delta}) \\ \times\tilde{h}^{\alpha}(\mathbf{p}_1,\omega_1)h^{\alpha}(\mathbf{p}-\mathbf{p}_1,\omega-\omega_1)h^{\beta}(\mathbf{p}_2,\omega_2)h^{\beta}(-\mathbf{p}-\mathbf{p}_2,-\omega-\omega_2)\,. \tag{A.16}$$

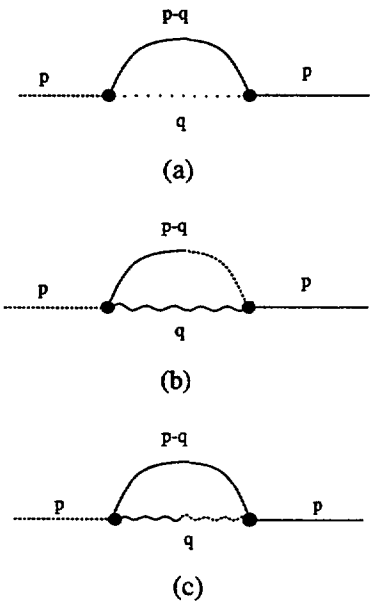

Fig. 5. — Diagramms contributing to the vertex function Γ_{11} of the undulation modes to one loop order ((a): $\Gamma_{11}^{(a)}$, (b): $\Gamma_{11}^{(b)}$, (c): $\Gamma_{11}^{(c)}$).

The resulting interaction part of the dynamic functional is then

$$J_{\text{eff}}^{\text{int}} = J_{\text{eff}}^{4\,\prime} + J_{\text{eff}}^{4a\prime} + J_{\text{eff}}^{4b}\,. \tag{A.17}$$

Now we start the diagrammatic analysis of this effective theory. The diagramms contributing to the vertex function Γ_{11} for the undulation modes are shown in figure 5.

$$\Gamma_{11}(\mathbf{p},\omega) = -i\omega + L_0 p^a \kappa_0 p^4 + \Gamma_{11}^{(a)} + \Gamma_{11}^{(b)} + \Gamma_{11}^{(c)} \tag{A.18}$$

The term $\Gamma_{11}^{(a)}$ reads

$$\Gamma_{11}^{(a)}(\mathbf{p},\omega) = L_0 p^a \int_{\mathbf{q}}\int_{\nu} \frac{4\mu_0(\mu_0+\lambda_0)}{2\mu_0+\lambda_0}(p^\alpha P_{\alpha\beta}^T(\mathbf{q})p^\beta)^2 C_h(\mathbf{p}-\mathbf{q},\omega-\nu)\,, \tag{A.19}$$

where $C_h(\mathbf{p},\omega)$ is the bare corrlation function given by

$$C_h(\mathbf{p},\omega) = \frac{2L_0 p^a}{\omega^2 + \Gamma_h(\mathbf{p}))^2}\,, \tag{A.20}$$

with the bare line width

$$\Gamma_h(\mathbf{p}) = L_0 p^a \kappa_0 p^4\,. \tag{A.21}$$

This contribution is frequency independent and leads to a renormalization of the bending rigidity κ_0. If the bare quantities are replaced by the fully renormalized terms this term is the dynamic generalization of the self consistent theory in reference [4]. The next two terms in equation (A.18) are frequency dependent and come from the phonon mediated effective 4-point vertices, equations (A.11,14),

$$\Gamma_{11}^{(b)}(\mathbf{p},\omega) = L_0^2 p^{2a} \int_{\mathbf{q}} \int_{\nu} \left[a^{\mathrm{T}}(\mathbf{p},\mathbf{q}) C_{\mathrm{u}}^{\mathrm{T}}(\mathbf{q},\nu) + a^{\mathrm{L}}(\mathbf{p},\mathbf{q}) C_{\mathrm{u}}^{\mathrm{L}}(\mathbf{q},\nu) \right] R_{\mathrm{h}}(\mathbf{p}-\mathbf{q},\omega-\nu)\,, \tag{A.22}$$

$$\begin{aligned}\Gamma_{11}^{(c)}(\mathbf{p},\omega) = L_0 p^a \int_{\mathbf{q}} \int_{\nu} \Big[& a^{\mathrm{T}}(\mathbf{p},\mathbf{q}) \left(D_0^{\mathrm{T}} q^a R_{\mathrm{u}}^{\mathrm{T}}(\mathbf{q},\nu) - \chi_{\mathrm{u}}^{\mathrm{T}}(\mathbf{q}) \right) + \\ & + a^{\mathrm{L}}(\mathbf{p},\mathbf{q}) \left(D_0^{\mathrm{L}} q^a (R_{\mathrm{u}}^{\mathrm{L}}(\mathbf{q},\nu) - \chi_{\mathrm{u}}^{\mathrm{L}}(\mathbf{q})) \right) \Big] C_{\mathrm{h}}(\mathbf{p}-\mathbf{q},\omega-\nu)\,,\end{aligned} \tag{A.23}$$

where

$$C_{\mathrm{u}}^{(\mathrm{L,T})}(\mathbf{q},\nu) = \frac{2 D_0^{(\mathrm{L,T})} q^a}{\nu^2 + (\Gamma_{\mathrm{u}}^{(\mathrm{L,T})}(\mathbf{q}))^2} \tag{A.24}$$

are the bare correlation functions of the phonon modes with the line widths

$$\Gamma_{\mathrm{u}}^{(\mathrm{L,T})}(\mathbf{q}) = D_0^{(\mathrm{L,T})} q^a \chi_{\mathrm{u}}^{(\mathrm{L,T})}(\mathbf{q})\,, \tag{A.25}$$

and the static susceptibilities $\chi_{\mathrm{u}}^{\mathrm{T}}(\mathbf{q}) = 1/\mu_0 q^2$, $\chi_{\mathrm{u}}^{\mathrm{L}}(\mathbf{q}) = 1/(\lambda_0 + 2\mu_0) q^2$. The response functions are defined by

$$R_{\mathrm{h}}(\mathbf{p},\omega) = \frac{1}{-i\omega + \Gamma_{\mathrm{h}}(\mathbf{p})}\,, \tag{A.26}$$

$$R_{\mathrm{u}}^{(\mathrm{L,T})}(\mathbf{p},\omega) = \frac{1}{-i\omega + \Gamma_{\mathrm{u}}^{(\mathrm{L,T})}(\mathbf{p})} \tag{A.27}$$

The vertex factors $a^{(\mathrm{L,T})}$ are given by

$$\begin{aligned}a^{(\mathrm{L,T})}(\mathbf{p},\mathbf{q}) = & \Big(\mu_0 \left[(\mathbf{q}\cdot\mathbf{p})(p-q)^l + (\mathbf{q}\cdot(\mathbf{p}-\mathbf{q}))p^l \right] + \lambda_0 (\mathbf{p}\cdot(\mathbf{p}-\mathbf{q}))q^l \Big) P_{lm}^{(\mathrm{L,T})}(\mathbf{q}) \\ & \Big(\mu_0 \left[(\mathbf{q}\cdot\mathbf{p})(p-q)^m + (\mathbf{q}\cdot(\mathbf{p}-\mathbf{q}))p^m \right] + \lambda_0 (\mathbf{p}\cdot(\mathbf{p}-\mathbf{q}))q^m \Big)\,.\end{aligned} \tag{A.28}$$

The diagrammatic contributions to the kinetic coefficient Γ_{20} are shown in figure 6.

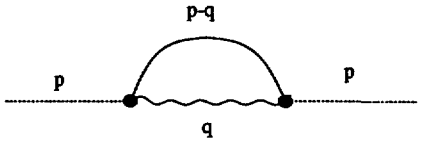

Fig. 6. — Diagramms contributing to the vertex function Γ_{20} of the undulation modes to one loop order ($\Gamma_{20}^{(a)}$).

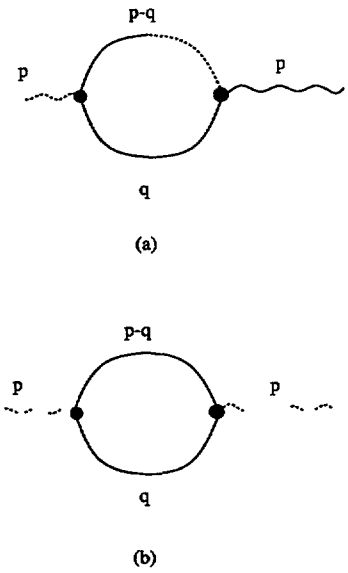

Fig. 7. — Vertex functions for the phonon modes renormalizing the effective phonon-mediated vertices ((a): $\Gamma_{11}^{lm}|_{mc}$, (b): $\Gamma_{20}^{lm}|_{mc}$).

$$\Gamma_{20}(\mathbf{p},\omega) = 2L_0 p^a + \Gamma_{20}^{(a)}\,, \tag{A.29}$$

where the mode coupling contribution is

$$\Gamma_{20}^{(a)}(\mathbf{p},\omega) = L_0^2 p^{2a} \int_{\mathbf{q}} \int_{\nu} \left[a^{\mathrm{T}}(\mathbf{p},\mathbf{q}) C_{\mathrm{u}}^{\mathrm{T}}(\mathbf{q},\nu) + a^{\mathrm{L}}(\mathbf{p},\mathbf{q}) C_{\mathrm{u}}^{\mathrm{L}}(\mathbf{q},\nu) \right] C_{\mathrm{h}}(\mathbf{p}-\mathbf{q},\omega-\nu)\,. \tag{A.30}$$

There is also a renormalization of the phonon modes due to insertions describing the decay into undulation modes. The corresponding vertex functions

$$\Gamma_{11}^{lm}(\mathbf{p},\omega)|_{\text{phonon}} = -i\omega + \Gamma_{11}^{lm}(\mathbf{p},\omega)|_{mc}\,, \tag{A.31}$$

$$\Gamma_{20}^{lm}(\mathbf{p},\omega)|_{\text{phonon}} = 2[D_0^{\mathrm{L}} P_{lm}^{\mathrm{L}}(\mathbf{p}) + D_0^{\mathrm{T}} P_{lm}^{\mathrm{T}}(\mathbf{p})] p^a + \Gamma_{20}^{lm}(\mathbf{p},\omega)|_{mc}\,, \tag{A.32}$$

are shown in figure 7. The mode coupling (mc) contributions are explicitly given by

$$\begin{aligned} \Gamma_{11}^{lm}(\mathbf{p},\omega)|_{mc} = p^a \int_{\mathbf{q}} \int_{\nu} \Big[& D_0^{\mathrm{T}} b^{\mathrm{T}}(\mathbf{p},\mathbf{q}) P_{lm}^{\mathrm{T}}(\mathbf{q}) + \\ & + D_0^{\mathrm{L}} b^{\mathrm{L}}(\mathbf{p},\mathbf{q}) P_{lm}^{\mathrm{L}}(\mathbf{q}) \Big] L_0 q^a R_{\mathrm{h}}(\mathbf{q},\nu) C_{\mathrm{h}}(\mathbf{p}-\mathbf{q},\omega-\nu)\,, \end{aligned} \tag{A.33}$$

$$\begin{aligned} \Gamma_{20}^{lm}(\mathbf{p},\omega)|_{mc} = p^{2a} \int_{\mathbf{q}} \int_{\nu} \Big[& (D_0^{\mathrm{T}})^2 b^{\mathrm{T}}(\mathbf{p},\mathbf{q}) P_{lm}^{\mathrm{T}}(\mathbf{q}) \\ & + (D_0^{\mathrm{L}})^2 b^{\mathrm{L}}(\mathbf{p},\mathbf{q}) P_{lm}^{\mathrm{L}}(\mathbf{q}) \Big] C_{\mathrm{h}}(\mathbf{q},\nu) C_{\mathrm{h}}(\mathbf{p}-\mathbf{q},\omega-\nu)\,. \end{aligned} \tag{A.34}$$

The vertex factors are defined by

$$b^{(L,T)}(\mathbf{p},\mathbf{q}) = \Big(\mu_0\left[(\mathbf{p}\cdot\mathbf{q})(p-q)^l + (\mathbf{p}\cdot(\mathbf{p}-\mathbf{q}))q^l\right] + \lambda_0(\mathbf{p}\cdot(\mathbf{p}-\mathbf{q}))p^l\Big) P_{lm}^{(L,T)}(\mathbf{p}) \Big(\mu_0\left[(\mathbf{p}\cdot\mathbf{q})(p-q)^m + (\mathbf{p}\cdot(\mathbf{p}-\mathbf{q}))q^m\right] + \lambda_0(\mathbf{p}\cdot(\mathbf{p}-\mathbf{q}))p^m\Big). \tag{A.35}$$

From the above equations one obtains a self consistent theory, if the bare correlation and response functions are replaced by the fully renormalized ones. This procedure corresponds to a resummation of certain diagramms in the perturbation series, including those for the renormalization of the phonon modes. Additionally one has to replace in the static quantities the elastic coefficients by their renormalized wave vector dependence, i.e., $\lambda_0 \to \lambda(q) = \lambda q^{\omega}$, $\mu_0 \to \mu(q) = \mu q^{\omega}$, and $\kappa_0 \to \kappa(q) = \kappa q^{2\zeta-2}$. Note that the vertex functions Γ_{11} and Γ_{20} are related to the correlation and response functions by

$$C(p,\omega) = \frac{\Gamma_{20}(p,\omega)}{\Gamma_{11}(p,\omega)\Gamma_{11}(-p,-\omega)}, \tag{A.36}$$

and

$$R(p,\omega) = \frac{1}{\Gamma_{11}(-p,-\omega)}. \tag{A.37}$$

References

[1] Proceedings of the Fifth Jerusalem Winter School, *Statistical Mechanics of Membranes and Surfaces*, Eds. Nelson D.R., Piran T. and Weinberg S., World Scientific (1989).
[2] Cates M.E., *Phys. Lett.* **161B** (1985) 363; *Phys. Rev. Lett.* **53** (1984) 926.
[3] Kantor Y., Kardar M. and Nelson D.R., *Phys. Rev. Lett.* **57** (1986) 791; Phys. Rev. A **35** (1987) 3056.
[4] Nelson D.R. and Peliti L., *J. Phys. France* **48** (1987) 1085.
[5] Paczuski M., Kardar M. and Nelson D.R., *Phys. Rev. Lett.* **60** (1988) 2638.
[6] Hohenberg P.C., *Phys. Rev.* **158** (1967) 383; Mermin N.D. and Wagner H., *Phys. Rev. Lett.* **17** (1966) 1133.
[7] Aronovitz J., Golubovic L. and Lubensky T.C., *J. Phys. France* **50** (1989) 609.
[8] David F. and Guitter E., *Europhys. Lett.* **5** (1988) 709.
[9] Aronovitz J. and Lubensky T.C., *Phys. Rev. Lett.* **60** (1988) 2634.
[10] Guitter E., David F., Leibler S. and Peliti L., *Phys. Rev. Lett.* **61** (1988) 2949; *J. Phys. France* **50** (1989) 1787.
[11] Kantor Y. and Nelson D.R., *Phys. Rev.* A **36** (1987) 4020.
[12] Plischke M. and Boal D., *Phys. Rev.* A **38** (1988) 4943.
[13] Ho J.-S. and Baumgärtner A., *Phys. Rev. Lett.* **63** (1989) 1324.
[14] Abraham F.F., Rudge W.E. and Plischke W., *Phys. Rev. Lett.* **62** (1989) 1757.
[15] Abraham F.F. and Nelson D.R., Science **249** (1990) 393; *J. Phys. France* **51** (1990) 2653.
[16] Alberts B., Bray D., Lewis J., Raff M., Roberts K. and Watson J.D., *The Molecular Biology of the Cell* (Garland, New York, 1983).
[17] Elgsaeter A., Stokke B., Mikkelsen A. and Branton D., *Science* **234** (1986) 1217.
[18] Schmidt C.F. and Svoboda K. (private communication);
See also Byers I.J. and Branton D., *J. Bacteriol.* **173** (1986) 933 and references therein.
[19] Beredjick N. and Burlant W.J., *J. Polymer Sci.* **A1** (8) (1970) 2807.
[20] Fendler J. H. and Tundo P., *Acc. Chem. Res.* **17** (1984) 3.

[21] Mutz M., Bensimon D. and Brienne M.J., *Phys. Rev. Lett* in press.
[22] Hwa T., Ph.D. Thesis, Physics Department, MIT (1990);Hwa T., Kokufuta E. and Tanaka T., MIT preprint; There is now Monte Carlo evidence (A. Baumgärtner, KF A Jülich preprint) that surfaces made of self-avoiding *plaquettes* can exist in a crumpled phase, in agreement with these experiments.
[23] Muthukumar M., J. Chem. Phys. **88** (1988) 2854 (1988); For a treatment of the dynamics of the crumpling transition, see Niel J., *Europhys. Lett.* **9** (1989) 415.
[24] Doi M. and Edwards S.F., *The Theory of Polymer Dynamics*, (Clarendon Press, Oxford, 1986).
[25] Rouse P.E., *J. Chem. Phys.* **21** (1953) 1272.
[26] Zimm B.H.,*J. Chem. Phys.* **24** (1956) 269 (1956).
[27] Kirkwood J.G. and Riseman J., *J. Chem. Phys.* **16** (1948) 565.
[28] Brochard F. and Lennon J.-F., *J. Phys. France* **36** (1975) 1690.
[29] See for instance Levich V.G., *Physiochemical Hydrodynamics*, (Prentice-Hall Inc., Englewood Cliffs, N.J., 1962).
[30] Lipowsky R. and Giradet M., *Phys. Rev. Lett.* **65** (1990) 2893.
[31] Janssen H.K., *Z. Phys.* **B 23** (1976) 377.
[32] de Dominicis C., *J. Phys. France* **37** (1976) Colloque C-247.
[33] Kawasaki K. and Gunton J.D., in *Progress in Liquid Physics*, ed. by C.A. Croxton, (Wiley, New York, 1978).
[34] Oono Y. and Freed K.F., *J. Chem. Phys.* **75** (1981) 1009.
[35] The solvent relaxation time τ_s for a flat membrane of size L is $\tau_s \sim L^2/\nu_0$. For $\nu_0 \approx 10^{-2} cm^2/sec$, the kinematic viscosity of water, this time is at least several orders of magnitude shorter than the internal membrane relaxation times calculated in this paper, for all $L \leq 10\mu$, which justifies the approximation (2.11). For *very* large surfaces ($L >> 10\mu$), however, the solvent relaxation time becomes comparable to these relaxations, and a new theory would be required.
[36] Halperin B.I., Hohenberg P.C. and Ma S., *Phys. Rev. Lett.* **29** (1972) 1548; Phys. Rev. **B 10** (1974) 139.
[37] Ma S. and Mazenko G.F., *Phys. Rev.* **B 11** (1975) 4077.
[38] Bausch R., Janssen H.K. and Wagner H., *Z. Phys.* **B 24** (1976) 113.
[39] Martin P.C., Siggia E.D. and Rose H.A., *Phys. Rev.* **A 8** (1973) 423.
[40] Abraham F.F., (unpublished).
[41] Hwa T., *Phys. Rev.* **A 41** (1990) 1751.
[42] Frey E., Doctoral thesis, Physik-Department der Technischen Universität München (1989);Frey E. and Schwabl F., to be published.
[43] Recall that m is the extension factor, i.e., the ratio between the actual linear size of the fluctuating membrane and its size at $T = 0$.
[44] Kirkwood J.G., *J. Polym. Sci.* **12** (1954) 1.
[45] de Gennes P.G., *Scaling Concepts in Polymer Physics*, (Cornell University, Ithaca, 1979).
[46] Nelson D.R., in *Phase Transitions and Critical Phenomena*, ed. by Domb C. and Lebowitz J.L., Vol.7, (Academic Press, 1983).
[47] Waugh R. and Evans E.A., *Biophys. J.* 26 (1979) 115.
[48] Evans E. and Skalak R., in *Mechanics and Thermodynamics of Biomembranes*, (CRC Press, Boca Raton, Fl., 1980).
[49] Browicz E., *Zbl. Med. Wiss.* **28** (1890) 625.
[50] Toner J., *Phys. Rev. Lett.* **64** (1990) 1741.
[51] Roux D. and Safinya C.R., *J. Phys. France* **49** (1988) 307.
[52] Larche F.C., Appell J., Pork G., Basserau P. and Marigenau J., *Phys. Rev. Lett.* **56** (1986) 1700.
[53] Mazenko G.F., Ramaswanny S. and Toner J.,*Phys. Rev.* **A 28** (1983) 1618.
[54] Zeman K., Engelhard H., Sackmann E., *Eur. Biophys. J.* **18** (1990) 203.
[55] Zeman K., Doctoral thesis, Physik-Department der Technischen Universität München (1989).